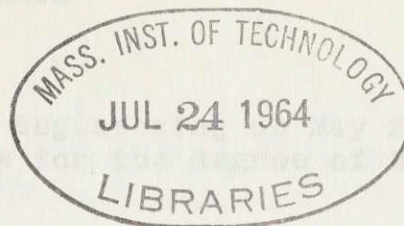


Submitted to the Department of Electrical Engineering in partial fulfillment of the requirements for the degree of Master of Science in Electrical Engineering.



A study is made of a novel type of antenna array excitation for possible use in radar and communication systems. The array excitations are unusual in that even at all the individual radiators of the array have an excitation completely different in frequency content. The broad class of antenna arrays which are called

**MULTIPLE-FREQUENCY ANTENNA ARRAYS**

by

**Terrence A. Lenahan**

By applying the method of plane wave analysis, an expression is derived for the radiation pattern of a multiple frequency array. The corresponding radiation pattern is constructed. This leads to the radiation pattern of an array for which the radiation distribution is shown that arrays may be designed to receive and

**SUBMITTED IN PARTIAL FULFILLMENT OF**

**THE REQUIREMENTS FOR THE DEGREE OF**

**MASTER OF SCIENCE IN ELECTRICAL ENGINEERING**

at the

**MASSACHUSETTS INSTITUTE OF TECHNOLOGY**

June, 1964

Once the general radiation pattern is determined the array directivity is analyzed. The relationship between directivity and the total broadside energy to the total excited array is determined. It is found that the multiple frequency array never makes full use of the directive potential of their array length, and in some cases they are non-directive arrays. The exact amount of directivity loss and a statement of joint angular-radial resolution for multiple frequency arrays is found in general terms.

Two practical techniques were examined in which the multiple frequency array might be used. The first, the time-integrating process makes use of a set of multiple frequency arrays to achieve a system with joint angular and radial resolution capability. Operational speed is sacrificed in this technique and it is shown that speed cannot be sacrificed directly by electronic scanning systems. The second processing technique involves the concept of a two-dimensional correlation function.

**Signature redacted**

Signature of Author

Department of Electrical Engineering, May, 1964

**Signature redacted**

Certified by

**Signature redacted**

Accepted by

Chairman, Departmental Committee on Graduate Students

Title: Professor of Electrical Engineering



by

038

TERRENCE ALBERT LENAHAN

Submitted to the Department of Electrical Engineering on May 28 in partial fulfillment of the requirements for the degree of Master of Science in Electrical Engineering.

A study is made of a novel type of antenna array excitation for possible use in radar and sonar systems. The array excitations are unusual in that some or all the individual radiators of the array have an excitation completely different in frequency content from other radiator excitations. The broad class of antenna arrays having excitations of this type are called "multiple frequency arrays".

By applying techniques of Fourier analysis, an expression is derived for the radiated energy distribution from the general one-dimensional multiple frequency array. Next the corresponding receiving array is defined and a receiving situation is constructed. This leads to an expression of the receiving characteristics of an array for which there is a certain equivalence with the radiation distribution of a transmitting array. In this way it is shown that arrays may be discussed independent of whether they transmit or receive energy.

Once the general relationship is established between the array excitation and the radiation distribution, the relationship is analyzed in terms of directivity and range resolution. Here directivity is measured by the ratio of the total broadside energy to the total emitted energy. Range resolution is measured by the localization of the pulse emitted in the broadside direction. It is found that the multiple frequency array never makes full use of the directive potential of their array length, and in some cases they are non-directive arrays. The exact amount of directivity loss and a statement of joint angular-radial resolution for multiple frequency arrays is found in general terms.

Two processing techniques were examined in which the multiple frequency array might be used. The first, the time-integration process makes use of a set of multiple frequency arrays to achieve a system with joint angular and radial resolution capability. Operational speed is sacrificed in this technique and it is shown that speed cannot be regained efficiently by electronic scanning schemes. The second processing technique introduces the concept of a two-dimensional correlation for achieving joint range-angle resolution capability from a non-directive multiple frequency array. The sacrifice here is equipment complexity arising from implementation of the two-dimensional correlator. This sacrifice is accentuated when Doppler effects are considered.

Thesis Supervisor: **Lan Jen Chu**

Title: **Professor of Electrical Engineering**



## FOOTNOTES

1. S. Silver, "Microwave Antenna Theory and Design", Radiation Laboratory Series No. 12, Mc-Graw Hill, New York, pp. 169-173; 1949.
  2. S. Silver, op cit, sec. 5.12, equation 107.
  3. S. Mason and H. Zimmerman, "Electronic Circuits, Signals, and Systems," John Wiley and Sons, New York; p. 236, equations 6.198 and 6.201; 1960.
  4. S. A. Schelkunoff and H. T. Friis, "Antennas Theory and Practice" John Wiley and Sons, New York; p. 182; 1952.
  5. E. Jahnke and F. Emde, Tables of Functions, Fourth Edition, Dover Publications, New York; pp. 34-37; 1945.
  6. S. Silver, op cit, p. 177.
  7. N. Wiener; "The Fourier Integral and Certain of its Applications"; Dover Publications, New York; p. 19; 1933.
  8. N. Wiener, op cit, p. 70.
  9. S. Mason, op cit, p. 236 equation 6. 198.
  10. The first formulation of the joint angle-range ambiguity function was by  
H. Urkowitz, C. Hauer, and J. F. Koval; "Generalized Resolution in Radar Systems"; Proceeds of the IRE, Vol.50, No. 10, 1960.  
The formulation here, which is more recent, was by  
T. K. Kashihara, "Investigation of Advanced Antenna Techniques", Philco Scientific Laboratory, Blue Bell, Pa., AF 19(628) -2403, Status Report 1; March, 1963.
  11. L. J. Cutrona, E. N. Leith, C. J. Palermo, and L. J. Porcello, "Optical Data Processing and Filtering Systems", IRE Transactions on Information Theory; June, 1960.
- P.20 \* Use upper signs when the angle is positive and lower signs when is negative.
- P.27 \* Recall from chapter two that the factor  $\lambda$  appears on reception whereas  $1/\lambda$  appears in the pattern on transmission. Therefore on measurement of the pattern this factor cancels.
- P.38 \* It was pointed out by L. J. Chu that implementation of the multiple frequency arrays will be hampered by mutual coupling effects which cannot be filtered out on transmission. This necessitates the use of shielding which otherwise could have been avoided.
- P.39 \* There has been electronic-scan receivers devised which by using FM signals avoid the necessity for time varying time delays. The efficient use of this scheme with the time integration scheme would invalidate this statement. This aspect has not been studied.

## CONTENTS

	Page
Abstract	2 - 2
List of Figures	5 - 5
Acknowledgements	6 - 6
Chapter	
I. Introduction	7 - 12
II. Pattern Derivations	13 - 17
III. Specific Patterns	18 - 25
A. Conventional Array	19 - 19
B. Linear Frequency Distribution	19 - 23
C. Symmetric Frequency Distribution	23 - 25
IV. Directivity	26 - 34
A. Composite Gain	27 - 28
B. Directive Gain	28 - 32
C. Joint Angular and Radial Resolution	32 - 34
V. Time-Integration Process	35 - 39
(Pattern Rotation)	38 - 39
VI. Ambiguity Function	40 - 46
(Implementation)	43 - 46
VII. Doppler Effects	47 - 49
VIII. Summary	50 - 52
Bibliography	53 - 53



## LIST OF FIGURES

	Page
1. Multiple Frequency Array Excitation Spectra	12a
2. Aperture Geometry	17a
3. Fresnel Integrals	20a
4. No-gain Multiple Frequency Array Pattern Plot	21a, 24a
5. High Gain Pattern with Excessive Sidelobes	26a
6. Composite Gain	28a
7. Good Resolution, Poor Localization	29a
8. Compensating Array Length	33a
9. Comparison with Fixed Array Length	34a
10. Multiple Frequency Array in Time-Integration Set	37a
11. Ambiguity Function Processor (optical)	46a
12. Ambiguity Function Processor (electronic)	46b



ACKNOWLEDGEMENT

I wish to acknowledge my indebtedness to Leo Procopio of the Philco Scientific Lab. The multiple frequency array and many of the subtopics in the paper are extensions of his original ideas. Also I would like to express my appreciation for stimulating conversations and helpful advice to Tom Kashiara and Peter Nave, also members of the Philco staff.

Finally, I am grateful to Professor Chu for his help in preparing this paper and his suggestions.

This work was done as a co-op student at the Philco Scientific Laboratory in Blue Bell, Pennsylvania.

The positions between the receiving elements. The network connections will be represented as a set of independent linear filters following each receiving element. The output of each filter will be attached to some summing device such that the output will be the sum of all the filter outputs.

Specifically, the excitations will be discussed in terms of the energy distribution radiated into space. For receiving arrays a point source emitting an impulse function will be postulated to exist in space. In such a case the output of the filter integrator can be written in terms of the impulse response of the filters and the location of the point source. On reception this integrator output will be the quantity of interest in this paper. The quantity may be thought of as the overall impulse response of the array with the point source location being a parameter.

Some assumptions will be made about the arrays



## CHAPTER I

## INTRODUCTION

An antenna array consists of a set of elements geometrically placed for either transmitting or receiving energy in some desired fashion. There are many features of an array, such as the type of elements, the location of the elements, and the network connecting the elements. For a transmitting array in this paper, the primary concern will be the excitation of each element. This excitation will be represented as a time function which depends on the element in question. For a receiving array in the paper, the primary concern will be the connections between the receiving elements. The network connections will be represented as a set of independent linear filters following each receiving element. The output of each filter will be attached to some summing device such that the output will be the sum of all the filter outputs.

Specifically, the excitations will be discussed in terms of the energy distribution radiated into space. For receiving arrays a point source emitting an impulse function will be postulated to exist in space. In such a case the output of the filter integrator can be written in terms of the impulse response of the filters and the location of the point source. On reception this integrator output will be the quantity of interest in this paper. The quantity may be thought of as the overall impulse response of the array with the point source location being a parameter.

Some assumptions will be made about the arrays



in this paper applying to transmit arrays and receiving arrays. First, the arrays will extend in one dimension over a straight line. Second, the elements comprising the array will be assumed to be non-directive. Finally the elements will be assumed to be very closely spaced. The first assumption results in a geometric simplification. The radiation distribution from a transmitting array will depend on only two position coordinates, as will the impulse response of a receiving array. The latter two assumptions allow an array to be approximated by a line, which on transmission will be a line source and on reception will be a continuum of filters. Thus some time functions continuously defined along the array will represent the excitation current. This may be written  $a(x,t)$  when  $x$  is the array coordinate and  $t$  is the time. Also some time function  $b(x',t)$  will represent the impulse response of the filter following the receiving element situated at the array position  $x'$ . This formulation incidentally is a generalization of the excitation or filtering of an array of discrete elements. On transmission for instance, the excitation of a discrete array can be written,  $a(x,t) = \sum_k \delta(x-x_k) S_k(t)$  where  $x_k$  is the  $k^{\text{th}}$  element location,  $S_k(t)$  is the corresponding excitation, and  $\delta(x)$  is the delta function.

Considering first transmitting arrays, a conventional array is defined as one having an a similar excitation, within an amplitude and phase factor, at each point of the array line. In general terms when  $a(x,t)$  is the excitation function, there will exist, for the conventional array, functions  $d(x)$  and  $c(t)$



such that  $a(x,t) = d(x) c(t)$ . Here  $d(x)$  represents the array illumination or amplitude and phase distribution over the array line; and  $c(t)$  is the modulation or the signal exciting each array point. In practice such an excitation is obtained by passing the signal  $c(t)$  through amplifiers having the gain,  $d(x)$ . The amplifier outputs lead to the corresponding array points.

This paper concerns arrays which for different array points have different excitations. These are the excitations which cannot be separated into the product of a time function and an illumination function. The class of arrays having such excitations will be called "multiple frequency arrays". For receiving arrays the distinction between multiple frequency and conventional arrays is made in terms of the impulse response of the filters following each receiving element. If  $b(x^1,t)$  represents this set of impulse responses, the conventional receiving array is one where  $b(x^1,t) = e(x^1) f(t)$  for some functions  $e$  and  $f$ . The multiple frequency receiving array is one having a filter function  $b(x^1,t)$  which cannot be written as the product of independent functions of time and array position. Again this non-separability of the function  $b(x^1,t)$  means that the impulse response of at least two filters is different.

The original motivation for studying the multiple frequency array arose in a radar and sonar application. The requirements of these systems is that targets or reflectors be reliably detected, located, and resolved in the presence of inter-

fering noise. Except in unusual circumstances, as discussed in Chapter 6, these requirements dictate that the

- (1) Propagated energy be concentrated in a small angular interval.
- (2) Propagated energy be concentrated at any given time in a small radial interval.
- (3) Impulse response energy of the receiving array be concentrated in a small interval of angles.
- (4) Impulse response energy of the receiving array be concentrated in a small interval of ranges.

Numbers (1) and (3) concern the directivity of transmitting and receiving arrays, respectively. Numbers (2) and (4) concern the respective range resolving capabilities of transmitting and receiving arrays. Taken together these conditions concern the joint range-angle resolution of a system.

In the particular application it was desired to transmit very high energy and wide band signals, at the same time achieving requirements (1) and (2). The multiple frequency array whose excitation spectrum is illustrated in figure 1a was suggested. Since the spectrum of the pulse, propagated in the broadside direction, consists of the excitation frequency content, a simple means of Fourier synthesizing the broadside pulse was presented by such an example. Thus the multiple frequency array of figure 1a can achieve an arbitrary broadside pulse, despite radiator or transmitter bandwidth limitations; whereas the conventional array will be affected by such limitations. It was felt that such bandwidth limitations may apply for high energy excitations. The disadvantage of using the array



excitation of figure 1a is a lack of directivity. This will be shown in chapters 3 and 4.

The question arises whether another type of multiple frequency array can achieve joint angular and radial resolution. Another question that arises is whether some appropriate processing scheme exists which can utilize the multiple frequency array of figure 1a to obtain good joint angular and radial resolution. The purpose of this thesis is to examine these two questions in detail.

The organization of the paper falls into three parts. The first is a derivation of the radiation distribution for the general excitation  $a(x,t)$ . The impulse response of the receiving array with filter function  $b(y,t)$  is also derived here. The important point of the second derivation states that the joint angle-range resolution of a receiving array depends on  $b(y,t)$  in the same way as joint transmission resolution depends on the excitation function  $a(x,t)$ . The second part of the paper formulates the joint resolution characteristics for an arbitrary multiple frequency array. In Chapter 4 a measure of antenna directivity and of range resolution capability are formulated. Then the relation between these two measures is derived in terms of the excitation function  $a(x,t)$ . The derived relation implies that given a total output bandwidth and a fixed array length, a conventional array achieves the greatest joint resolution capability. The multiple frequency array, consequently always has worse directivity. Figure 1b and 1c show the frequency content of some arbitrary multiple frequency arrays for which the results in

Chapter 4 apply. In particular the results show quantitatively just how much directivity is lost for each array.

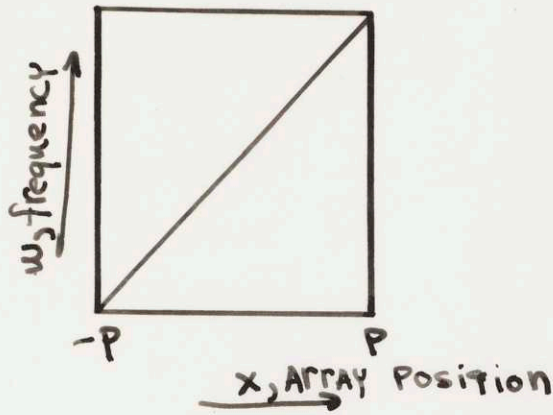
Processing techniques which circumvent the directivity problems of multiple frequency arrays form the subject of the final part. The first technique, called the time-integration process, utilizes a combination of multiple frequency arrays. These arrays are picked so that when combined by this process they cause the effect of a wide-band conventional array. It is found that a set of monochromatic conventional arrays combined in the same way introduces two interesting contrasts. For only the conventional arrays, RF phase is important; but these arrays are more amenable to electronic pattern rotation. The second technique is based on a transformation of what is called the two-way pattern. The two-way pattern is usually the final processed signal of a radar system. It is found that use of the transformation results in a system of good joint resolution when an array excitation of the type in figure 1a is used. The drawback of the system is the necessary equipment complexity for realizing the transformation. This drawback becomes worse still when doppler effects are considered, as shown in the sixth and seventh chapter.



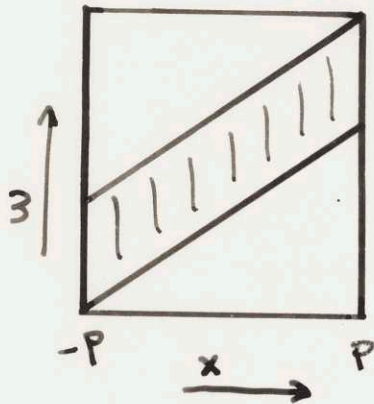
Figure 1

12a.

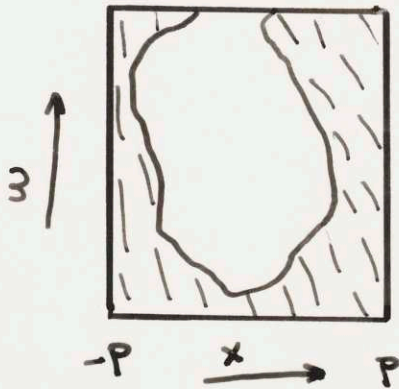
a.



b.



c.



Multiple Frequency Array Excitations (spectra)

## CHAPTER 2

## PATTERN DERIVATIONS

The expression for an antenna excitation over the  $xy$  plane will be  $a(x,y,t)$  where for any point  $(x,y)$ , the time function  $a(x,y,t)$  has finite energy. From this excitation it is desired to find, as a function of location and time, the radiated energy intensity. This is done by extending a result of Silver's to find the radiation field or pattern. The squared modulus of the pattern <sup>is</sup> proportional to the radiated energy distribution.

Considering the aperture  $P$  to be in the  $xy$  plane, Silver's result concerns the single frequency excitation,  $F(x,y) e^{j\omega_0 t}$ . He found that the resulting radiated field can be written, (1) (2.1) 
$$U = \frac{j\omega_0 e^{j\omega_0(t - \frac{R}{c})}}{4\pi c R} \iint_P F(x,y) (\cos\theta + i_z \cdot S) e^{j\frac{\omega_0}{c} \sin\theta (x\cos\phi + y\sin\phi)} dx dy$$
 The geometry of the situation is expressed by the spherical coordinates  $(R, \phi, \theta)$  and the rectangular coordinates  $(x,y,z)$  shown in figure #2. Other symbols include the time  $t$ , the propagation velocity  $c$ , and the phase factor  $i_z \cdot S$  which can be taken to be constant. (2) In arriving at (2.1) three approximations were made,

1. Linear and uniform polarization.
2. Excitation wavelength  $<$  aperture dimensions.
3. Far field,  $R \gg$  aperture dimensions.

None of these restrict the application of (2.1) in this paper.

The frequency content of the excitation  $a(x,y,t)$  is given by its Fourier transform, which is written

$$(2.2) \quad A(x,y,\omega) = \int_{-\infty}^{\infty} a(x,y,t) e^{-j\omega t} dt$$



Isolating one spectral component in the excitation spectrum, one can apply Silver's result to give the spectral density of the radiation field for that component. Thus

$$(2.3) \quad U(\omega_0) = \iint_P \frac{\cos\theta + \beta}{4\pi c R} j\omega_0 e^{-j\omega_0 \frac{R}{c}} A(x, y, \omega) e^{j\frac{\omega_0}{c}(x \cos\phi + y \sin\phi)} dx dy$$

Since superposition is valid the total radiation field is

$$(2.4) \quad U = \int_{-\infty}^{\infty} U(\omega) e^{j\omega t} \frac{d\omega}{2\pi} = \frac{\beta + \cos\theta}{4\pi c R} \int_{-\infty}^{\infty} \iint_P j\omega A(x, y, \omega) e^{j\omega(t - \tau_{xy})} dx dy \frac{d\omega}{2\pi}$$

where

$$(2.5) \quad \tau_{xy} = \frac{R}{c} - \frac{x}{c} \sin\theta \cos\phi - \frac{y}{c} \sin\theta \sin\phi$$

After inverting the order of integration in (2.4), the interior actually is the inverse transform of the quantity  $j\omega A(x, y, \omega) e^{-j\omega \tau_{xy}}$ . This is  $\frac{\partial}{\partial t} a(x, y, t - \tau_{xy})$ <sup>(3)</sup>. Thus an equivalent expression

for the radiation field from the excitation  $a(x, y, t)$  is

$$(2.6) \quad U = \frac{\beta + \cos\theta}{4\pi c R} \iint_P \frac{\partial}{\partial t} a(x, y, t - \tau_{xy}) dx dy$$

For facility in manipulation, the full generality of

(2.6) will not be used, and only one dimensional arrays will be considered. This means that the excitation is written,

$$(2.7) \quad a(x, y, t) = a(x, t) \delta(y)$$

and the radiation field outside the  $XZ$  plane can be deduced from symmetry, so the angle  $\phi$  is set to zero. The resulting field expression is

$$(2.8) \quad U = \frac{\beta + \cos\theta}{4\pi c R} \int_{-P}^P \frac{\partial}{\partial t} a(x, t - \tau_x) dx = \frac{\beta + \cos\theta}{4\pi c R} \int_{-P}^P \int_{-P}^P j\omega A(x, \omega) e^{j\omega(t - \tau_x)} dx \frac{d\omega}{2\pi}$$

where

$$(2.9) \quad \tau_x = \frac{R}{c} - \frac{x}{c} \sin\theta$$

The case of the two-dimensional aperture can be handled as a straight forward extension of the one-dimensional case for any

of the topics in the paper.

The field expression in (2.8) may be interpreted physically as a sum of aperture pointsources appropriately delayed and regulated by the energy propagation factor  $\frac{1}{4\pi R}$  and the obliquity factor  $\beta + \cos\theta$ . The time derivative indicates the transformation from aperture excitations into fields in space. On reception the opposite effect occurs, for then the effective area varies as the reciprocal of the squared frequency with respect to power received. <sup>(4)</sup> Therefore when many frequencies are present, the incoming field pulse is actually integrated.

The characteristics of the receiving array depend upon this integration effect as will be shown. Suppose that the receiver filters are given by  $a(x,t)$  and postulate a point field source at  $(R_0, \theta_0)$  emitting a delta function. By (2.8), this field corresponds to the point source current excitation,  $cu_1(t)\delta(R-R_0, \theta-\theta_0)$  where  $U-1(t)$  is the unit step  $(u_1(t) = \int_{-\infty}^t \delta(t) dt)$ . (Note that the obliquity factor does not arise for a point source). Now reciprocity can be applied; for the process of transmission is reciprocal, within a time derivative, to the process of reception. On transmission the current excitation  $a(x,t)$  can be achieved by exciting by a delta function, filters having the impulse response  $a(x,t)$  leading to point  $x$ . On reception the delta-function current excitation is applied to some arbitrary point in space, which before was used for measuring purposes. The received signal is measured at the same place the transmitter is excited.

where  $A(x, \omega)$  and  $B(y, \omega)$  are the Fourier transforms of  $a(x, t)$  and



Suppose the transmission field at  $(R_0, \theta_0)$  is  $U$ , then the induced current on the measuring point is  $c \int_{-\infty}^{\infty} U(t) dt$ . By reciprocity the received signal from the filter integrator for the unit step will be  $c^2 \int_{-\infty}^{\infty} ds \int_{-\infty}^{\infty} U(l) dl$ . Thus for a delta-function pointfield source the receiver signal will be, by (2.8)

$$(2.10) \quad U' = \frac{(B + \cos \theta) c}{4\pi R} \int_{-\infty}^{\infty} \int_{-P}^P a(x, l - \tau_x) dx dl$$

This will be named the received field.

It should be noted that when currents are measured in the radiation field the derivative in (2.8) will disappear. Also when a delta-function point current source is postulated on reception, the time integral in (2.10) will disappear.

For radar and sonar applications an expression for a third type of pattern, known as the "two-way pattern", is desired. The two-way pattern is a combination of the transmission and reception patterns which gives the final processed signal in terms of

1. Transmitting array excitation,  $a(x, t)$ .
2. Receiving array filters,  $b(x^1, t)$
3. Location  $(R, \theta)$  of a reflecting point target.

Assume for mathematical convenience that the transmitter and receiver are superimposed in the array interval  $(-p, p)$ . Then the derivation of the two-way pattern is based on the fact that for any single frequency, the corresponding two-way pattern is the product of the transmit and receiver patterns. Thus if

$$(2.10) \quad V(\omega_0) = \frac{(\cos \theta + \beta_r)(\cos \theta + \beta_t)}{(4\pi c R)^2} \int_{-P}^P A(x, \omega_0) e^{-j\omega_0 \tau_x} dx \int_{-P}^P B(x', \omega_0) e^{j\omega_0 \tau_{x'}} dx'$$

where  $A(X, W)$  and  $B(x', w)$  are the Fourier transforms of  $a(x, t)$  and

*Figure 2*

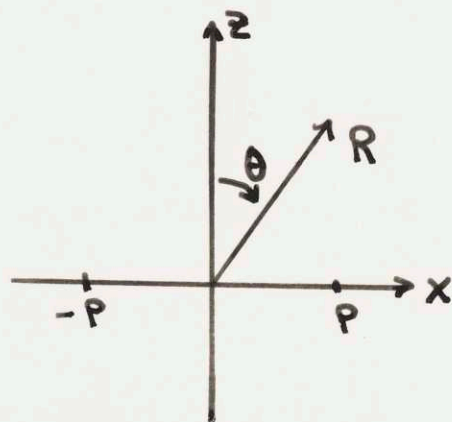
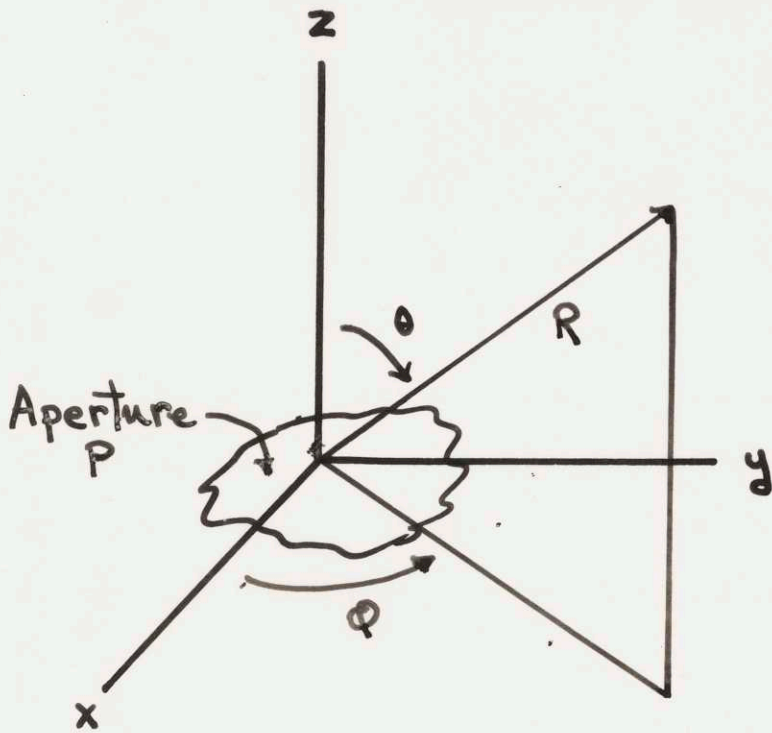
$b(x',t)$  respectively. Notice that the factor  $j\omega$  has canceled upon multiplication of the patterns. Employing the superposition principle, one obtains for the total two-way pattern, when  $C(R,\theta)$  represents the obliquity and radial factors,

$$(2.11) \quad V = \int_{-\infty}^{\infty} V(\omega) e^{j\omega t} \frac{d\omega}{2\pi} = C(R,\theta) \int_{-\infty}^{\infty} \int_{-P}^P A(x,\omega) B(x',\omega) e^{j\omega(t - \frac{2R}{c} + \frac{x+y}{c} \sin\theta)} dx dy \frac{d\omega}{2\pi}$$

If it is desired to express  $V$  in terms of  $a(x,t)$  and  $b(x',t)$ , note that (2.11) is the Fourier transform of the product of two quantities. Consequently  $V$  is the convolution of their Fourier transforms; so the two-way pattern is the convolution of the transmit and receive patterns. There will be occasion to use the two-way pattern after the transmit pattern has been discussed in some detail.

*Aperture Geometry*





One-dimensional ARRAY

Aperture Geometry

## CHAPTER 3

## SPECIFIC PATTERNS

In this chapter suppose that the excitation function has the form

$$(3.1) \quad a(x, t) = a(x) e^{j\omega(x)t}$$

which represents those arrays whose radiators are excited by the single frequency given by  $\omega(x)$ . Such a class of excitations has a simplified expression for the radiated field, and yet it is still general enough to include many different types of excitations. In particular arrays where  $\omega(x) = \text{constant}$  are conventional arrays, and arrays where  $\omega(x)$  is different for each  $x$  (as in figure 1a) are the extreme multiple frequency array where no frequency is duplicated in the excitation spectrum.

Substitution of (3.1) into (2.8) yields the radiation field,

$$(3.2) \quad U = \frac{\cos\theta + B}{4\pi c R} \frac{d}{dt} \int_{-P}^P a(x) e^{j\omega(x)(t - \frac{R}{c} + \frac{x}{c} \sin\theta)} dx$$

On the basis of the discussion in the preceding chapter the quantity,

$$(3.3) \quad Q = \int_{-P}^P a(x) e^{j\omega(x)(t - \frac{R}{c} + \frac{x}{c} \sin\theta)} dx$$

contains the information of how the excitation affects the radiation systems, and the time derivative, as in 2.10, cancels upon measurement of the field. Consequently attention will be focused on the quantity  $Q$ , which will be called the pattern.

The purpose of this chapter is to examine the patterns



of three different excitations. From the analysis trends will be pointed out whose generalization will be the subject of the succeeding chapter.

#### A. Conventional Array

When  $W(x) = W_0$ , some constant, the excitation corresponds to that of a conventional array. The pattern becomes,

$$(3.4) \quad Q = e^{j\omega_0(t - \frac{R}{c})} \int_{-P}^P a(x) e^{j\frac{\omega_0 x}{c} \sin \theta} dx$$

When  $a(x) = 1$ ,

$$(3.5) \quad Q = 2P e^{j\omega_0(t - \frac{R}{c})} \frac{\sin(\frac{\omega_0 P}{c} \sin \theta)}{\frac{\omega_0 P}{c} \sin \theta}$$

In either case the pattern has no dependence, other than phase, on the range  $R$ .  $Q$  does vary with the angle  $\theta$ , and in (3.5) the variation is quite distinctive. For large values of  $W_0 P$  the great majority of radiated energy lies in an angular distance of  $\frac{2\pi c}{\omega_0 P}$  about the broadside direction ( $\theta = 0$ ). Thus the angular energy concentration or directivity of this pattern improves without limit as the factor  $W_0 P$  becomes large. For different angular shaped patterns, different functions  $a(x)$  are required. The contract which can be drawn is to a hypothetical point source emitting some spectrum  $b(w)$ . Here there will be no angular dependence of the radiation field, and the radial pulse can be arbitrarily specified for the proper function  $b(w)$ .

#### B. Linear Frequency Distribution

Suppose for a second example that

$$(3.6) \quad w(x) = \omega_0 (1 + \delta x/p) \quad (-P \leq x \leq P)$$

When  $a(x) = 1$ , the radiation pattern is given by

$$(3.7) \quad Q = \int_{-P}^P e^{j\omega_0(1 + \delta x/p)(t - R/c + x/c \sin \theta)} dx$$

This integration is most easily performed by letting

$$(3.8) \quad A = \frac{P}{2\delta} - \frac{R - ct}{2 \sin \theta}, \quad B = \frac{\omega_0 \delta}{pc} \sin \theta$$

then substituting into (3.7) to give

$$(3.9) \quad Q = \int_{-P}^P e^{j\omega_0(t-\frac{R}{c})} e^{jB(x^2 + 2xA + A^2)} e^{-jBA^2} dx$$

A change of variables,  $S = x + A$ , brings the reduction,

$$(3.10) \quad Q = e^{j\omega_0(t-\frac{R}{c})} e^{-jBA^2} \int_{-P+A}^{P+A} e^{jBS^2} ds \\ = e^{j\omega_0(t-\frac{R}{c})} e^{-jBA^2} \int_{-P+A}^{P+A} (\cos BS^2 + j \sin BS^2) ds$$

Expressions of the form,  $\int_0^u \sin \frac{\pi}{2} t^2 dt$  and  $\int_0^u \cos \frac{\pi}{2} t^2 dt$  are known as Fresnel integrals which are tabulated functions. (5)

By denoting these,  $S(u)$  and  $C(u)$ , respectively, the final pattern expression is

$$(3.11) \quad Q = e^{j\omega_0(t-\frac{R}{c})} e^{-jBA^2} \sqrt{\frac{\pi}{2|B|}} \left\{ C[(P+A)\sqrt{\frac{2|B|}{\pi}}] \right.$$

$$\left. - C[(A-P)\sqrt{\frac{2|B|}{\pi}}] + j S[(P+A)\sqrt{\frac{2|B|}{\pi}}] \pm j S[(A-P)\sqrt{\frac{2|B|}{\pi}}] \right\}^*$$

The case when  $B = 0 = \theta$  must be handled separately. Refer to

(3.7), then by setting  $\theta = 0$ , one obtains for the broadside field,

$$(3.12) \quad Q = e^{j\omega_0(t-\frac{R}{c})} \int_{-P}^P e^{j\frac{\omega_0 \delta}{P} x(t-\frac{R}{c})} dx \\ Q = 2P e^{j\omega_0(t-\frac{R}{c})} \frac{\sin \omega_0 \delta (t-R/c)}{\omega_0 \delta (t-R/c)}$$

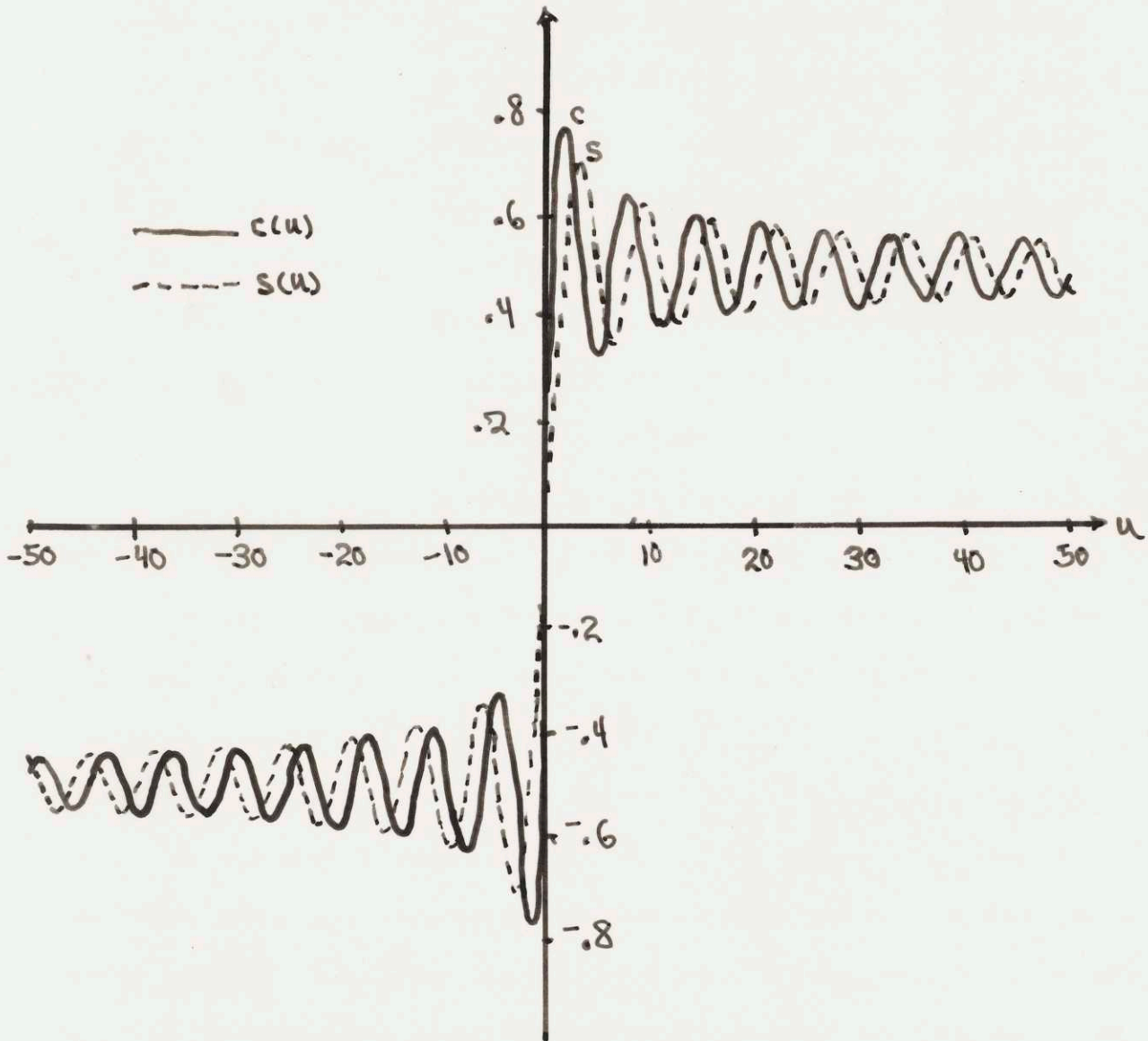
Expressions (3.11) and (3.12) describe completely and exactly

the radiation pattern for the linear frequency distribution case.

An interpretation of the pattern must be based on the nature of Fresnel integrals which are plotted in figure #3. Both functions are antisymmetric and hence intersect the origin. They have a damped oscillatory behavior about the values  $1/2$  or  $-1/2$ , depending on the argument sign, and they approach these values for large arguments. The asymptotic forms are given by

$$(3.13) \quad C(x) \approx \frac{1}{2} + \frac{1}{x\pi} \sin \frac{\pi}{2} x^2 \\ S(x) \approx \frac{1}{2} - \frac{1}{x\pi} \cos \frac{\pi}{2} x^2$$





Fresnel Integrals

With the assumption that  $\frac{Pw_0\delta}{c} = 40\pi$  and  $\delta = .2$ , the pattern has been plotted in figure #4a. The outstanding feature of the plot is a maximal ridge located on the locus given by  $R = ct + \frac{P}{\delta} \sin\theta$ , and known as a Limacon. The ridge is maximal in the sense that for a fixed angle  $\theta$  and time  $t$ , the pattern intensity for ranges  $R$  off the Limacon is less than that on the Limacon. Hence the collection of radial maxima indexed by  $\theta$  may be said to specify the Limacon. In this respect the plotted example is a good indication of the general character of (3.11) and (3.12) because such a ridge appears in the pattern for all values of  $P, \delta$ , and  $W_0$ .

The existence of such a ridge may be deduced from (3.9). Fixing the angle  $\theta$  and time  $t$ , the expression is maximized for  $A = 0$ , which is just the locus equation for the Limacon. To find the pattern on the ridge, set  $A = 0$  in (3.11) to give

$$(3.14) \quad Q_r = 2P e^{jw_0(t - \frac{R}{c})} \sqrt{\frac{\pi}{2|B|P^2}} \left[ C\left(\sqrt{\frac{2|B|P^2}{\pi}}\right) + jS\left(\sqrt{\frac{2|B|P^2}{\pi}}\right) \right]$$

The important parameter here is  $\frac{2|B|P^2}{\pi} = \frac{2Pw_0\delta|\sin\theta|}{\pi c}$ . When the parameter equals zero, ie  $\theta = 0$ ,  $Q_r$  has the maximum value  $2p$ ; and large values of the parameter result in small values of the pattern intensity. The pattern for intermediate values of the parameter is described by the half power points of the ridge. These points lie within the interval

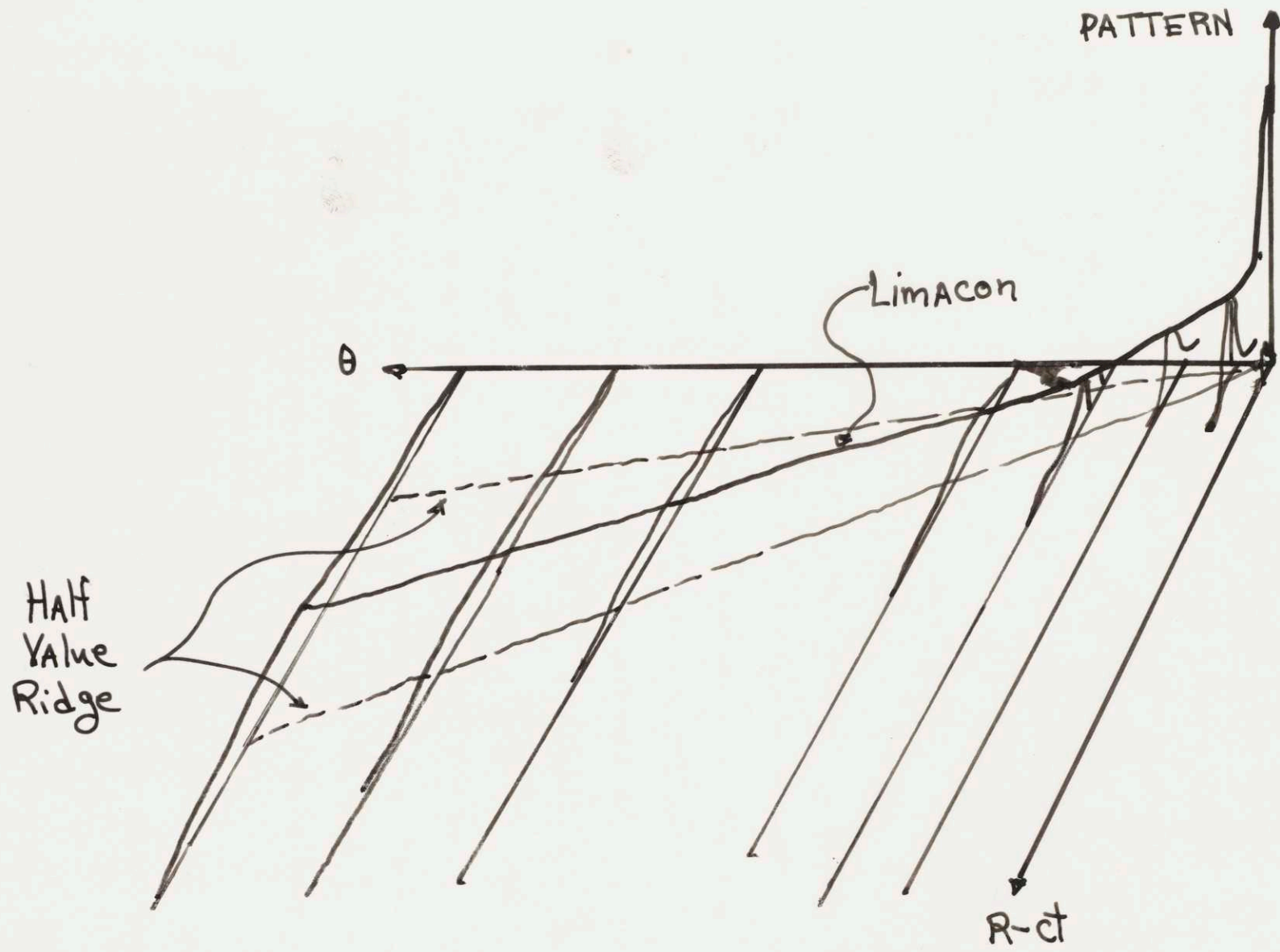
$$\left( \theta = -\frac{\pi c}{Pw_0\delta}, \theta = +\frac{\pi c}{Pw_0\delta} \right)$$

This value is verified by first setting  $\theta = \frac{\pi c}{Pw_0\delta}$  and observing that  $\frac{2|B|P^2}{\pi} > 2$ . Then,

$$(3.15) \quad |Q_r| \cong 2P\sqrt{\frac{1}{2}} |C(\sqrt{2}) + jS(\sqrt{2})| < 2P\sqrt{\frac{1}{2}}$$

as a reference to the Fresnel integral tables will show. Thus the pattern on the Limacon can be arbitrarily localized or peaked





No - Gain Multiple Frequency Array  
 Pattern Plot

Figure 4a.

21a.

by either increasing the bandwidth,  $W_0\delta$ , or the array length,  $2P$ .

Examination of the radial pulses in the pattern for an arbitrary and fixed  $\theta$  and  $T$  shows that the total energy within each pulse is independent of  $\theta$ . Since it just has been shown that the pulse maxima decrease with increasing  $\theta$ , it follows that the radial pulses must broaden for increasing  $\theta$ . A quantitative derivation of this phenomena appears in a more general context in the next chapter. A qualitative appreciation of the broadening affect can be gained here by locating two half-value ridges, where for a fixed angle and time the pattern intensity is half of that on the maximal ridge. It will be shown that these ridges diverge for increasing angle  $\theta$ , which implies that the pulses do broaden. The ridges are located on the loci  $A = \pm P$  or  $R = ct + (\frac{P}{\sin\theta} \pm P) \sin\theta$

because the corresponding pattern expression there is

$$(3.16) \quad |Q_{nl}| = P \sqrt{\frac{\pi}{2|B|P^2}} \left| C\left(\sqrt{\frac{2|B|P^2}{\pi}}\right) \mp S\left(\sqrt{\frac{2|B|P^2}{\pi}}\right) \right|$$

which is approximately half of  $Q_r$ , when  $\frac{2|B|P^2}{\pi}$  is not small.

This observation depends on the fact that the Fresnel integrals vary little for arguments removed from zero. The radial distance between the two half-value ridges is  $4a \sin\theta$ , which increases as  $\theta$  increases. Therefore the ridges do diverge and the radial pulse broadening is shown.

Outside the region between the half-value ridges, the behavior of the pattern may be deduced from the asymptotic forms of the Fresnel integrals. From expressions,

(3.11) and (3.12), it follows that for large values of  $R-ct$ ,

$$(3.17) \quad |Q| \leq \sqrt{\frac{\pi}{2|B|}} \frac{2 \cdot 2}{\pi A \sqrt{\frac{2|B|}{\pi}}} = \frac{2}{A|B|} \sim \frac{4Pc}{W_0\delta} \frac{1}{R-ct}$$



Hence the pattern decreases from its maximum at a rate comparable to  $\frac{1}{R-ct}$  for increasing values of  $R-ct$ ; Consequently a large percentage of the radiated energy lies between the half-value ridges.

### C. Symmetric Frequency Distribution

The previous examples represented the extremes in frequency distributions, with complete frequency duplication along the array excitation in (A.) and no frequency duplication in (B.) The symmetric multiple frequency distribution is a compromise between the two extremes where  $w(x) = \omega_0(1 + \frac{\delta}{p}|x|)$  for  $-P \leq x \leq P$ . Thus a band of frequencies is represented and each particular frequency in the excitation appears twice along the array.

Again assume  $a(x) = 1$ , then the pattern will be given by

$$(3.18) \quad Q = \int_{-P}^P e^{j\omega_0(1 + \frac{\delta}{p}|x|)(t - \frac{R}{c} + \frac{x}{c} \sin \theta)} dx$$

By expanding the expression and changing the integration variable, one obtains

$$(3.19) \quad Q = \int_0^P e^{j\omega_0(1 + \frac{\delta}{p}x)(t - \frac{R}{c} + \frac{x}{c} \sin \theta)} dx + \int_0^P e^{j\omega_0(1 + \frac{\delta}{p}x)(t - \frac{R}{c} - \frac{x}{c} \sin \theta)} dx$$

Let  $A' = \frac{P}{2\delta} + \frac{R-ct}{2 \sin \theta}$ , then after using the definitions, (3.8) and the manipulations of example B, (3.19) becomes

$$(3.20) \quad Q = e^{j\omega_0(t - \frac{R}{c})} \left[ e^{j\delta A'^2} \int_A^{P+A} e^{j\delta y^2} dy + e^{-j\delta A'^2} \int_{A'}^{P+A'} e^{-j\delta y^2} dy \right]$$

The pattern envelope obeys the inequality

$$(3.21) \quad |Q| \leq \left| \int_A^{P+A} e^{j\delta y^2} dy \right| + \left| \int_{A'}^{P+A'} e^{-j\delta y^2} dy \right|$$

These two integrals are similar to the ones of example B, so expression (3.21) can be interpreted in terms of the results of Section B.

The pattern envelope is bounded by the sum of two patterns respectively having maximal ridges on the loci,

$$(3.22) \quad R = ct + \left(P + \frac{P}{\delta}\right) \sin\theta \quad \text{or} \quad A = -\frac{P}{2}$$

$$R = ct - \left(P + \frac{P}{\delta}\right) \sin\theta \quad \text{or} \quad A' = -\frac{P}{2}$$

The radial pulses centered about each ridge remain essentially independent except for small angles  $\theta$ . The corresponding half value ridges are separated by  $2P\sin\theta$  whereas the maximal ridges are separated by  $2\left(P + \frac{P}{\delta}\right)\sin\theta$ . Therefore, the ridge values reinforce each other only on broadside, and the energy content of the radial pulses will be greatest for that direction.

Again the case where  $\theta = 0$  must be handled separately.

Setting  $\theta = 0$  in (3.19) results in

$$(3.23) \quad Q = 2e^{j\omega_0\left(t - \frac{R}{c}\right)} \int_0^P e^{j\frac{\omega_0\delta}{P}x\left(t - \frac{R}{c}\right)} dx$$

$$= 2Pe^{j\omega_0\left(t - \frac{R}{c}\right)} \frac{\sin \frac{\omega_0\delta}{2}\left(t - \frac{R}{c}\right)}{\omega_0\delta/2\left(t - \frac{R}{c}\right)}$$

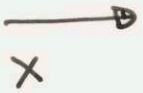
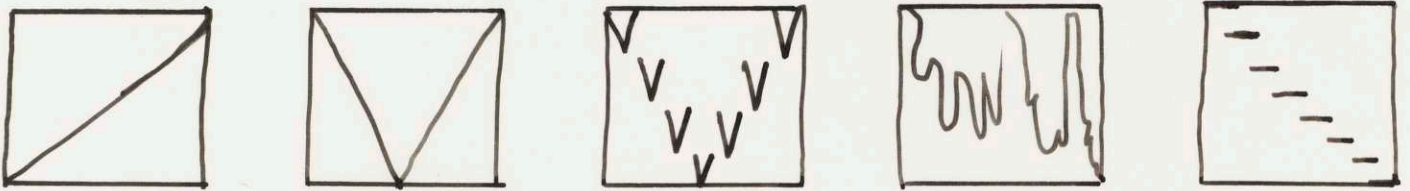
This broadside pulse is broader by a factor of two compared to (3.12). Thus this pattern compared to that of example B is more localized in an angular way, but the broadside pulse is broader and hence less localized.

On the basis of the examples in this chapter, there seems to be greater angular localization of the pattern when more frequencies are duplicated along the array excitation. Also the radial localization of the broadside pulse is greater when a wider band of frequencies is used. Other excitations with the form  $a(x)e^{jw(x)t}$ , as in figure #4b, could be analyzed to show similar trends. It is desired, however, to establish a more precise formulation of pattern directivity and range resolution



Figure 4b.

24a.



Other Examples of Excitations of the Form,  
 $a(x)e^{j\omega(x)t}$

capability. Finally the relation, if any, between these two qualities is desired for determining the joint angle and range resolution of an antenna array. This more general subject is discussed in the next chapter.

The gain of a conventional array has been used to indicate the power gain between the antenna and a point for a given input power; and also it provides a coarse measure of pattern directivity. When the array has a uniform phase distribution and an excitation,  $a(x)$ , the gain is defined as

$$(4.1) \quad G = \frac{\int_{-\lambda_0/2}^{\lambda_0/2} |a(x)|^2 dx}{\int_{-\lambda_0/2}^{\lambda_0/2} |a(x)|^2 dx}$$

where  $\lambda_0$  is the corresponding wavelength. This ratio compares the maximum power (on broadside) to the total transmitted power. Hence large gain values indicate a predominance of broadside power over the average transmitted power. Occasionally a high gain antenna pattern could have enough total power outside the main beam to exceed the power in the main beam. Such a pattern appears in Figure 23. Therefore gain provides only a coarse measure of directivity.

Since multiple frequency array patterns have radial as well as angular dependence, a single measure of directivity for them disregards radial dependence. Consequently to fill the two previous needs of gain two gain generalizations have been formulated. The first specifies the peak power density between the antenna and a point for a given total input energy. This is called composite gain. The



## CHAPTER 4

## PATTERN DIRECTIVITY

The gain of a conventional array has been used to indicate the power passing between the antenna and a point for a given input power; and also it provides a coarse measure of pattern directivity. When the array has a uniform phase distribution and an excitation,  $a(x)e^{j\omega t}$ , the gain is defined as<sup>(6)</sup>

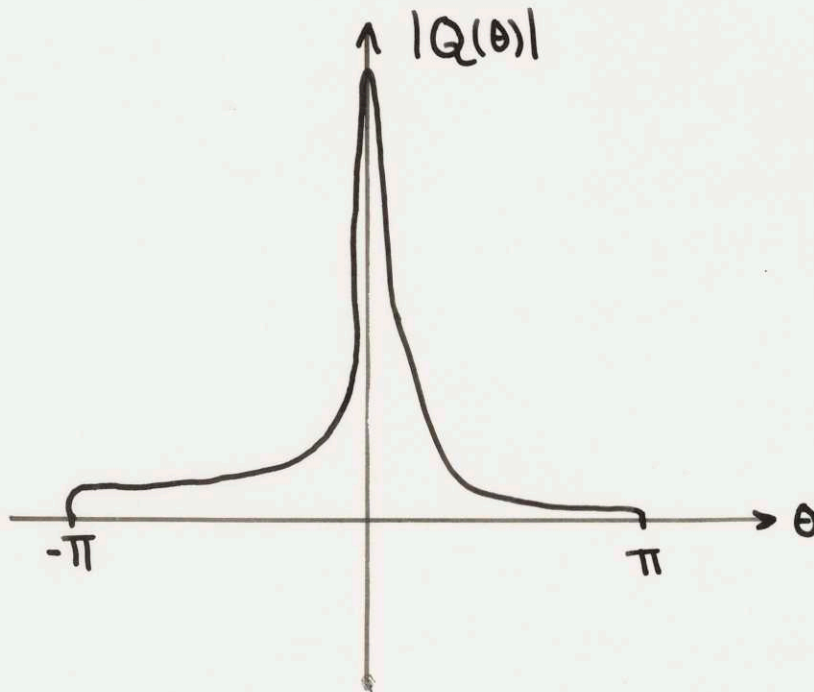
$$(4.1) \quad G' \equiv \frac{\left| \frac{2}{\lambda_0} \int_{-P}^P a(x) dx \right|^2}{\int_{-P}^P |a(x)|^2 dx}$$

where  $\lambda_0$  is the corresponding wavelength. This ratio compares the maximum power (on broadside) to the total transmitted power. Hence large gain values indicate a predominance of broadside power over the average transmitted power taken over <sup>All directions</sup>  $\lambda$ . Conceivably a high gain antenna pattern could have enough total power outside the main beam to exceed the power in the main beam. Such a pattern appears in figure #5. Therefore gain provides only a coarse measure of directivity.

Since multiple frequency array patterns have radial as well as angular independence, a single measure of directivity for them disregards even more pattern information than before. Consequently to fill the two previous needs of gain two gain generalizations have been formulated. The first specifies the peak power passing between the antenna and a fixed point for a given total input energy. This is called composite gain. The

Figure 5

26a.



Pattern with excessive sidelobe energy,  
but high gain.



second gain provides a coarse measure of pattern directivity, and so it is called directive gain.

### A. Composite Gain

Using (2.8) and the considerations leading to (3.3) the pattern corresponding to the excitation  $A(x, \omega)$  is defined

$$(4.2) \quad Q(\theta, t - \frac{R}{c}) = \int_{-\infty}^{\infty} \int_{-P}^P A(x, \omega) e^{j\omega(t - \frac{R}{c} + \frac{x}{c} \sin\theta)} dx \frac{d\omega}{2\pi}$$

Assume the phase distribution over the aperture is uniform so that the maximum pattern strength lies on broadside at  $R = ct$ .

In this case composite gain is defined,

$$(4.3) \quad G_c \equiv \frac{\left| \int_{-\infty}^{\infty} \int_{-P}^P A(x, \omega) dx \frac{d\omega}{2\pi} \right|^2}{\int_{-\infty}^{\infty} \int_{-P}^P |A(x, \omega)|^2 dx \frac{d\omega}{2\pi}} \sim \frac{\text{Peak pattern power}}{\text{Total pattern energy}}$$

Note that this formulation has left out the obliquity effect, which previously resulted in a factor of two, and the factor  $\lambda$ . Consequently this form is equally applicable to transmission and reception, and the numerator is proportional by a factor of four to the measured peak power.\*

There is a geometric analog where  $1/G_c$  represents a cross-sectional area of the pattern. Correspondingly, the quantity  $\int_{-\infty}^{\infty} \int_{-P}^P |A(x, \omega)|^2 dx \frac{d\omega}{2\pi}$  is the total volume (energy) and the quantity  $\left| \int_{-\infty}^{\infty} \int_{-P}^P A(x, \omega) dx \frac{d\omega}{2\pi} \right|^2$  is the maximum height (peak power). This analog serves to illustrate the fact that the composite gain is independent of pattern shape. For example the point source emitting the spectrum,  $a(\omega)$ , and the monochromatic conventional array with illumination  $a(x)$  both have the composite gain given by

$$(4.4) \quad G_c = \frac{\left| \int_{-P}^P a(x) dx \right|^2}{\int_{-P}^P |a(x)|^2 dx}$$

The relation between the excitation and composite gain is elucidated by the example where

$$(4.5) \quad A(x, w) = E \text{ or Zero, depending on } X \text{ and } W.$$

Then

$$(4.6) \quad \int_{-\infty}^{\infty} \int_{-P}^P |A(x, w)|^2 dx dw = E \int_{-\infty}^{\infty} \int_{-P}^P A(x, w) dx dw$$

and so

$$(4.7) \quad G_c = \int_{-\infty}^{\infty} \int_{-P}^P \frac{A(x, w)}{E} dx \frac{dw}{2\pi}$$

This expression represents the area in the frequency-position plane for which the excitation is non-zero. Figure #6 illustrates the situation. When the output bandwidth is  $B$  for each position  $X$ , this area is  $2PB$ . This conclusion could also have been reached by using Schwartz's inequality <sup>(7)</sup> to give,

$$(4.8) \quad \left| \int_B \int_{-P}^P A(x, w) dx \frac{dw}{2\pi} \right|^2 \leq 2PB \int_B \int_{-P}^P |A(x, w)|^2 dx \frac{dw}{2\pi}$$

where now  $B$  is the total output bandwidth. This implies

$$(4.9) \quad G_c \leq 2PB$$

with equality when  $A(x, w) = \text{constant}$  for  $-P \leq x \leq P$  and  $w \in B$ .

This means that the composite gain is maximized, for a certain bandwidth  $B$  and array length  $2p$ , when the excitation is uniform over these. Therefore, a measure of the affected area in the frequency-position plane has been constructed where points are weighted with respect to their relative energy contributions.

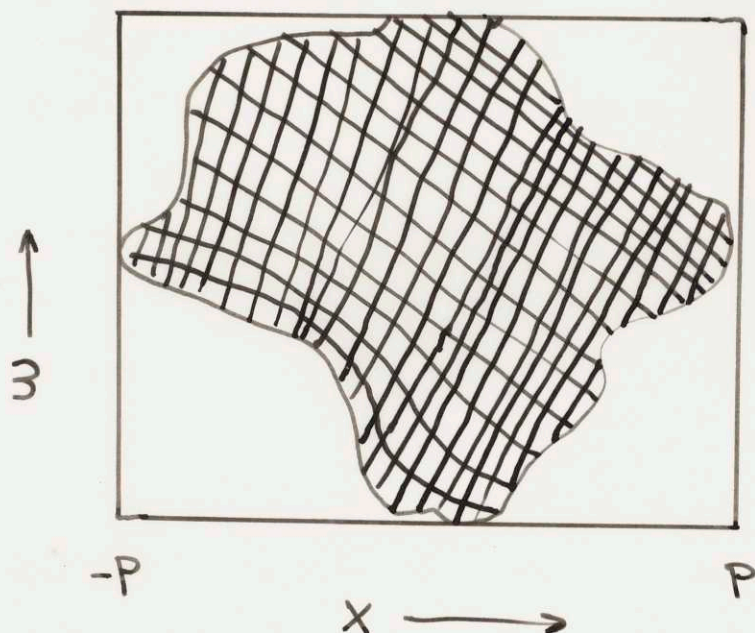
### B. Directive Gain

When  $A(x, w)$  is the excitation of an array, and  $Q(\theta, t - \frac{R}{c})$  is the resulting pattern, directive gain is defined,

$$(4.10) \quad G_d \equiv \frac{\int_{-\infty}^{\infty} |Q(\theta, t - \frac{R}{c})|^2 dt - \frac{R}{c}}{\int_{-\infty}^{\infty} \int_{-P}^P |A(x, w)|^2 dx \frac{dw}{2\pi}} \quad || \frac{\text{Broadside energy}}{\text{Total pattern energy}}$$

Again the obliquity factor and the time derivative in the field expression, (2.8), are neglected. Therefore the numerator in





Each point in the crosshatched region represents a non-zero frequency component at a certain array position.  $G_c$  is the area of that region when the excitation is uniform over it.

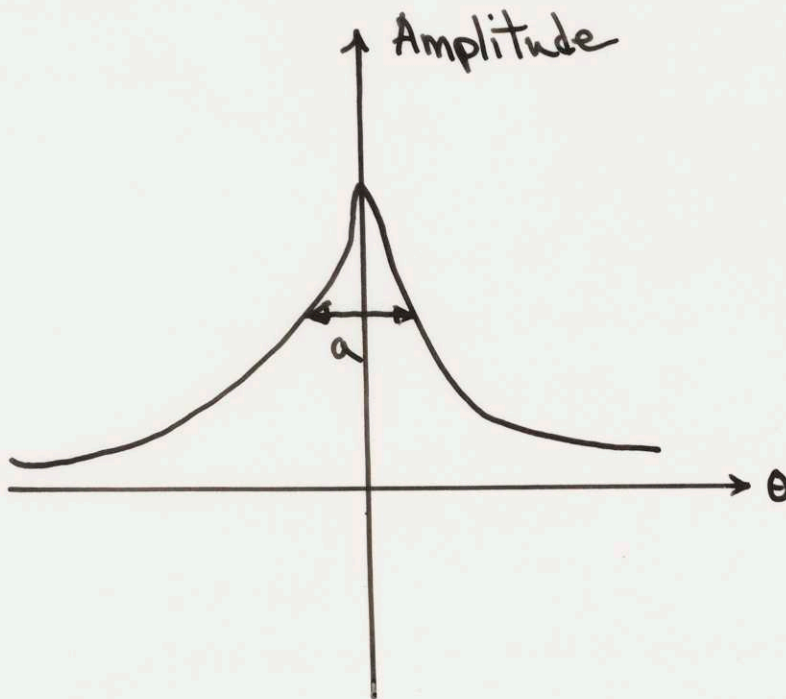
COMPOSITE GAIN

(4.10) is proportional to the total measured broadside energy with a proportionality factor of four. This factor is not essential for it can just be recalled when necessary.

It is essential to state in what sense directive gain is a good or useful measure of pattern directivity. For this purpose the concept of localization and resolution capability are introduced. Localization, in this paper, concerns the extent to which energy is distributed, either in space or time. As a one-dimensional example, when the maximum value and total energy of a pulse are given, the pulse of greatest localization is the rectangular pulse. Resolution capability, in this paper, refers to the facility with which a pulse is distinguished when a shifted version of the same pulse is added. Thus resolution may be measured by the distance between the half power points of a pulse. With the constraints of the previous example, it can be seen that the rectangular pulse represents almost the worst resolution situation. Figure #7 shows cases of much better resolution, and indeed, at the expense of localization, the resolution can be arbitrarily good with the constraints given.

In viewing the pattern  $Q(\theta, \tau - \frac{R}{c})$  as a set of radial pulses indexed by the angle  $\theta$ , a function  $E(\theta)$ , can be defined which gives the total energy in a pulse as a function of the angle. The maximum value of  $E(\theta)$ , at  $\theta = 0$ , is the numerator of (4.10), and the total pattern energy, which is  $\int_0^{2\pi} E(\theta) d\theta$ , is the denominator. Hence the quantity  $1/Gd$  may be considered the width of a





Good resolution, poor localization.

rectangular pulse having height  $E(0)$  and total energy  $\int_0^{2\pi} E(\theta) d\theta$  so  $1/G_d$  represents the greatest localization of the function  $E(\theta)$  and approximately the worst resolution. Typically for pattern synthesis, a worst localization of  $E(\theta)$  could be specified, and this would then immediately specify a lower bound requirement for  $G_d$ . Also a resolution requirement leads to some sufficient value of  $G_d$ .

On the other hand, no matter how large the directive gain of a pattern becomes, there is no assurance that

- (1) Localization will be adequate
- (2) All small energy, big amplitude spots are eliminated. Such anomalies, if reflected, would confuse a threshold receiver.

Hence directive gain may be useful as a necessary directive condition, but never as a sufficient one. Recourse must always be made to the pattern to obtain sufficient directivity conditions.

The relation between directive gain and the excitation can be elucidated by first considering arrays with unit (no) gain. Suppose for all frequencies  $w$ ,

$$(4.11) \quad A(x_1, w) A(x_2, w) = 0 \quad \text{when} \quad x_1 \neq x_2$$

In words this means that no two array points have any frequency components in common. By Parseval's Theorem, (8)

$$(4.12) \quad \int_{-\infty}^{\infty} |Q(0, t - \frac{R}{c})|^2 dt = \int_{-\infty}^{\infty} \left| \int_{-P}^P A(x, w) dx \right|^2 \frac{dw}{2\pi}$$

Expanding the integral, then applying (4.11), one obtains

$$(4.13) \quad \int_{-\infty}^{\infty} \left| \int_{-P}^P A(x, w) dx \right|^2 \frac{dw}{2\pi} = \int_{-\infty}^{\infty} \int_{-P}^P |A(x, w)|^2 dx \frac{dw}{2\pi}$$

therefore by (4.10)

$$(4.14) \quad G_d = 1$$



for these excitations. Thus the multiple frequency array whose excitation spectrum has no frequency duplications along the array propagates an equal amount of energy in all directions (neglecting the obliquity factor). Note that the shape of the radial pulses need not be the same for all directions, but the energy therein is the same. The second example in the preceding chapter is such a no-gain multiple frequency array.

For antenna excitations which do achieve some directivity, a relation holds between  $G_d$  and the gains of the conventional arrays comprising the particular excitation. Define the gain of the  $w$ -frequency by

$$(4.15) \quad G_w \equiv \frac{\left| \int_{-P}^P A(x, w) dx \right|^2}{\int_{-P}^P |A(x, w)|^2 dx}$$

where as usual  $\frac{2}{\lambda}$  has been eliminated from (4.1).

Hence by (4.10) and (4.12),

$$(4.16) \quad G_d = \frac{\int_{-\infty}^{\infty} G_w \int_{-P}^P |A(x, w)|^2 dx dw}{\int_{-\infty}^{\infty} \int_{-P}^P |A(x, w)|^2 dx dw}$$

This implies that directive gain is an average of the various conventional gains. The average is such that each  $G_w$  is weighted by the total energy transmitted at its particular frequency. When

$\int_{-P}^P |A(x, w)|^2 dx$  is uniform over  $w$ , the directive gain is just the mean of the  $G_w$ . In the previous example  $G_w = 1$  for each  $w$ , so  $G_d$  had to equal 1. For the third example of the preceding chapter, directivity was present; and the amount is that of a dipole since each represented frequency occurs in the excitation twice along the array. Similarly the directive gain of any mul-



multiple frequency array can be found as an average gain of its constituent conventional arrays.

### C. Joint Angular and Radial Resolution

The first step in describing joint resolution properties is to determine the relation between range resolution and the excitation. As seen in the last chapter the emerging broadside pulse is narrow when the total excitation bandwidth is large. Generally, a bandwidth measure indicates range resolution capability. If bandwidth is defined as the difference between the highest and lowest frequencies, however, there will be no distinction between the spectrum whose energy is equally distributed and one whose energy is concentrated into a small part of the band. This is relevant to range resolution, for the former example must yield a narrow broadside pulse, and the latter pulse need not be narrow.

Instead, an effective bandwidth is defined to be

$$(4.17) \quad B_e \equiv \frac{\left| \int_{-\infty}^{\infty} \int_{-P}^P A(x, \omega) dx \frac{d\omega}{2\pi} \right|^2}{\int_{-\infty}^{\infty} \left| \int_{-P}^P A(x, \omega) dx \right|^2 \frac{d\omega}{2\pi}} = \frac{\text{Peak broadside power}}{\text{Total broadside energy}}$$

This definition is the same type as for  $G_d$ , for  $1/B_e$  represents the length of the rectangle of height  $\left| \int_{-\infty}^{\infty} \int_{-P}^P A(x, \omega) dx \frac{d\omega}{2\pi} \right|^2$  and total energy  $\int_{-\infty}^{\infty} \left| \int_{-P}^P A(x, \omega) dx \right|^2 \frac{d\omega}{2\pi}$ . In other words  $1/B_e$  represents the greatest localization and nearly the worst resolution of the broadside pulse with antenna excitation  $A(x, \omega)$ .

Assuming that  $A(x, \omega)$  is restricted to some bandwidth  $B$ , apply Schwartz's inequality to (4.17) to obtain

$$(4.18) \quad B_e \leq \frac{\left| \int_B \int_{-P}^P A(x, \omega) dx \frac{d\omega}{2\pi} \right|^2}{\frac{1}{B} \int_B \left| \int_{-P}^P A(x, \omega) dx \right|^2 \frac{d\omega}{2\pi}} = B$$



with equality when the quantity  $\left| \int_{-P}^P A(x, \omega) dx \right|^2$  is constant for all  $\omega$  in the band. Thus the effective bandwidth,  $B_e$  measures the bandwidth of the broadside pulse taking into account the relative energy contribution of each frequency component.

From the expressions in (4.17), (4.10) and (4.12), and (4.3) follows the statement of joint angle and range resolution

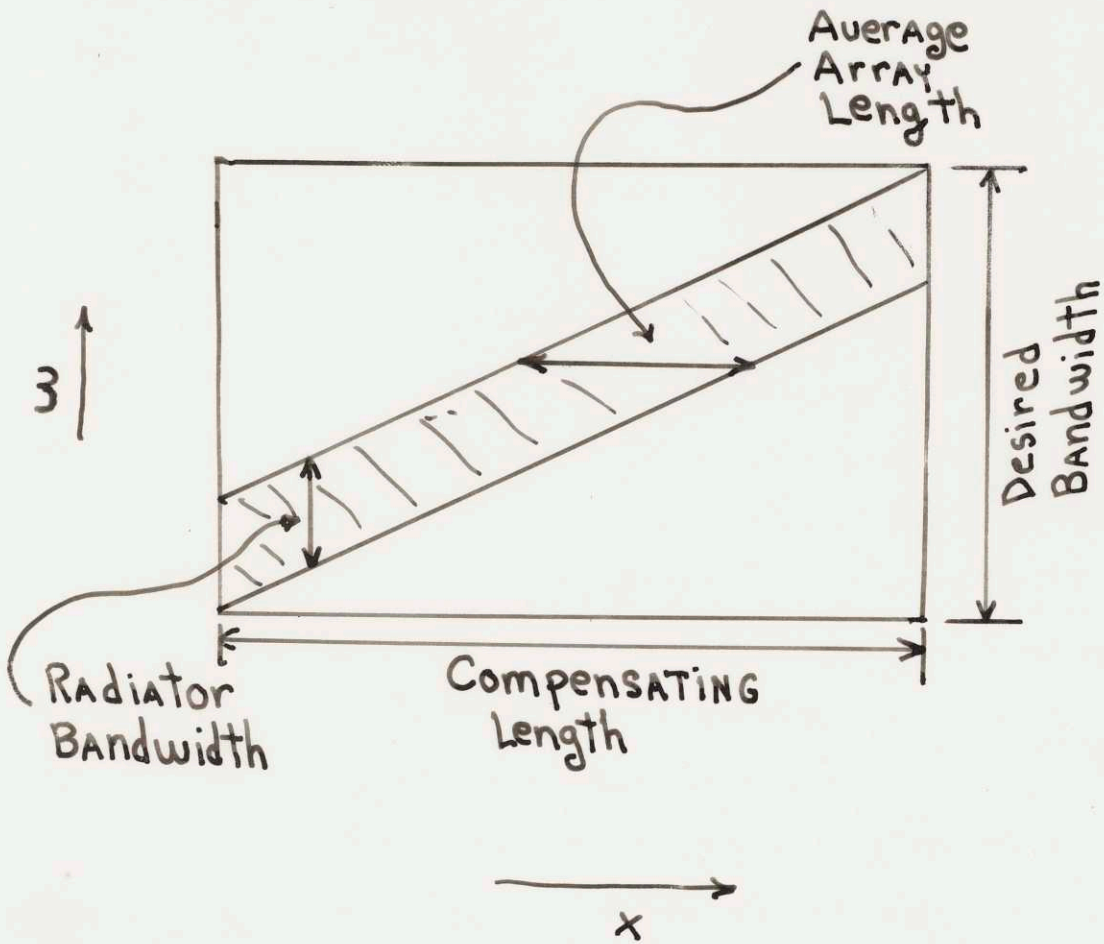
$$(4.19) \quad G_d B_e = G_c$$

Hence when the composite gain is specified, a tradeoff between directivity and range resolution will arise. In that case the effective bandwidth can only be increased at the expense of directive gain, and vice versa. For example, the three arrays of the preceding chapter have the same composite gain, which is given by (4.4), and it was pointed out there how directivity and range resolution were being traded.

In practice the composite gain may or may not be constrained. When for instance the radiators are each capable of emitting the desired total output bandwidth and the array length is adequate, the composite gain has no limitations within the context of the problem. The design procedure insures the proper  $B_e$  by having each radiator bandwidth equal  $B_e$ . By having each radiator band the same, the proper  $G_d$  is ensured. Thus such a situation calls for a conventional array where directivity and range resolution are separate notions. When the radiator bandwidths are limited below the desired output bandwidth, a multiple frequency array excitation, like that in figure #8, is called for. The resulting pattern will have a loss in directivity according to (4.19), un-

Figure 8

33a.



COMPENSATING ARRAY LENGTH

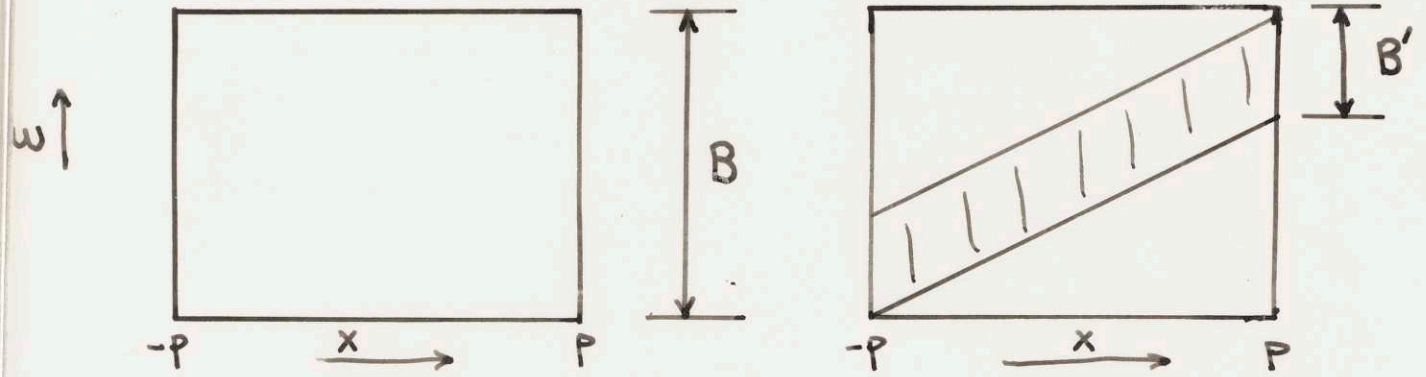


less the total array length is increased. The effective array length of each frequency is hereby restored to the desired value, which also restores the composite gain to its desired value.

On the other hand when the array length is limited, a multiple frequency array with the same effective bandwidth as some conventional array makes less efficient use of the potential directivity in the array. The multiple frequency array has a smaller  $G_c$  in this case, so that the value of  $G_d$  is smaller and hence the directivity is not as good. Therefore, the multiple frequency array, by reducing the effective array length corresponding to each frequency, meets a reduction in directivity compared to the corresponding conventional array. Figure #9 illustrates this comparison.

The rest of the paper concerns some sacrifices which can be made in various systems to overcome the directivity problem. In each case the system involves a change of emphasis from the antenna pattern to some other quantity where the tradeoff of (4.19) is deemphasized. In chapter 5, this quantity is a combination of patterns, and in chapter 6, this quantity is a transformation of a pattern.

COMPARISON BETWEEN ARRAYS  
ASSUMING FIXED ARRAY LENGTH



Conventional Array

$$G_c = 2PB$$

$$G_d = 2P$$

$$B_e = B$$

Multiple-Frequency Array

$$G_c = 2PB'$$

$$B_e = B$$

$$G_d = 2P \frac{B'}{B} < 2P$$

COMPARISON BETWEEN ARRAYS,  
ASSUMING FIXED ARRAY LENGTH.



## CHAPTER 5

## TIME - INTEGRATION PROCESS

The time-integration process is a technique which facilitates the use of high energy or wide band antenna excitations. The fundamental idea behind the method is a decomposition into small subsets of the total energy or bandwidth to be transmitted, whereupon these small subsets are excited separately in time. As examples these subsets may be smaller power levels or smaller frequency bands of the excitation. The receiver of the system collects the various transmitted energy packets (which may or may not have been reflected as incommunication), then by appropriate delays the packets can be combined into their original form. By linearity the final combined result will be identical to that had all the subsets been transmitted simultaneously. Hence the scheme is a spreading of the total energy or bandwidth to be transmitted over time which thereby reduces the power or bandwidth requirements of the radiators.

In particular the time-integration process will be applied to give the result of a wide-band conventional array by the use of monochromatic conventional arrays or no-gain multiple frequency arrays. In either case bandwidth limitations of the individual radiators are avoided since any radiator emits only one frequency at a time. The purpose of this chapter is to describe the time integration process and to show the relative advantages of either type of array.

Suppose for this chapter that the arrays consist of discrete radiators, each of which emit discrete frequency components. Let these frequency components be given by

$$(5.1) \quad \omega_n = \omega_0 \left(1 + \frac{n\delta}{N}\right) \quad -N \leq n \leq N$$

and let the corresponding amplitude and phase of the excitation and filter be  $a_{nm}$  and  $b_{nl}$  respectively. The  $m^{\text{th}}$  radiator position and the  $l^{\text{th}}$  filter position are given by

$$(5.2) \quad x_m = md \quad \text{AND} \quad x'_l = ld \quad -M \leq m, l \leq M$$

where  $d$  is the element separation for the transmitting and receiving arrays and  $\frac{\omega_0\delta}{N}$  is the frequency spacing. By (2.11) the two-way pattern for the system is

$$(5.3) \quad V = C(R, \theta) \sum_{-N}^N \sum_{-M}^M \sum_{-M}^M a_{nm} b_{nl} e^{j\omega_n \left[ t - \frac{2R}{c} + \frac{x_m + x'_l}{c} \sin\theta \right]}$$

As the first illustration of the time integration process, suppose only one frequency component of the excitation is emitted at a given time. Once all the possible reflected returns are back from one component, the next is excited, and so on until all components have been excited. The return from the  $n^{\text{th}}$  component is

$$(5.4) \quad V_n = C(R, \theta) \sum_m \sum_l a_{nm} b_{nl} e^{j\omega_n \left[ t_n - \frac{2R}{c} + \frac{x_m + x'_l}{c} \sin\theta \right]}$$

where  $t_n = t - (N + n)\tau$  and  $\tau$  is the time between various component excitations. Delaying  $V_n$  by  $(N + 1 - n)\tau$  then summing over  $n$  yields

$$(5.5) \quad \sum_n V_n = V \left( t - (2N + 1)\tau \right)$$



This is the two-way pattern of a conventional array with bandwidth  $2W_0\delta$ . In order to obtain this result, however, it was necessary to account for the RF phase of the returns. Such implementation is impractical.

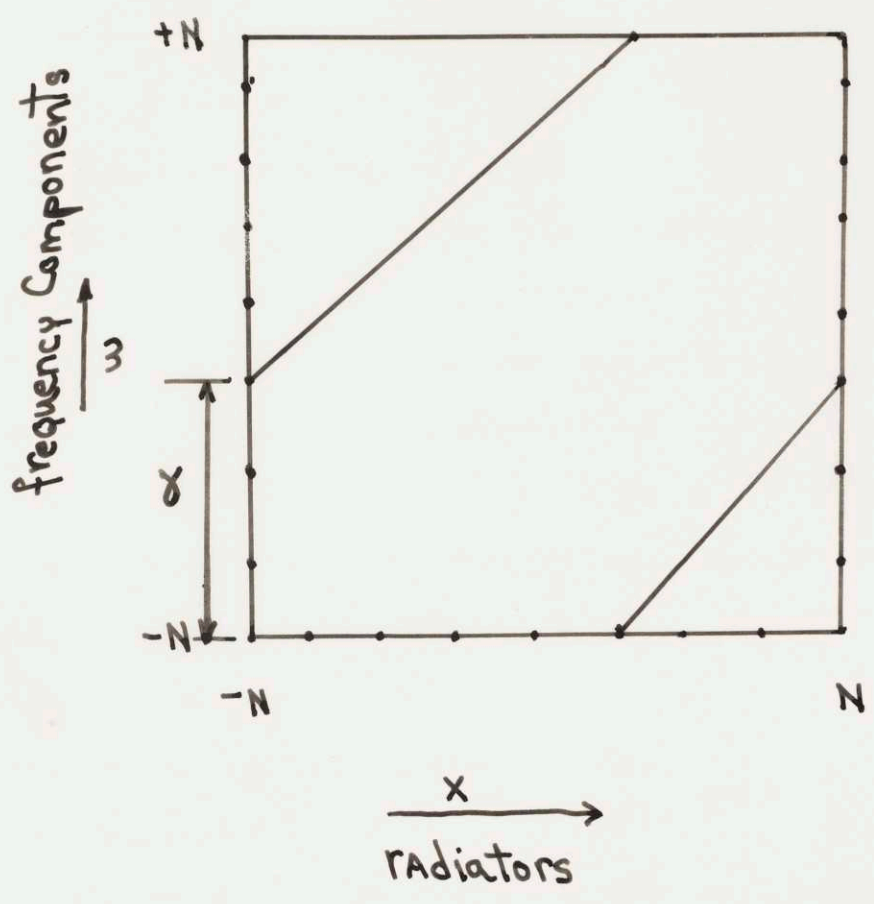
Upon applying the time-integration process to multiple frequency arrays, the RF phase of the returns becomes unimportant. Basically this follows from the joint range and angle variation of their pattern. Define the set of excitations as follows:

Each frequency component of (5.1) is transmitted for each member array. They by letting  $M = N$  above, a single and different frequency is emitted by each radiator in each member array. Therefore each member array is a no-gain multiple frequency array. To distinguish the members, there is the requirement that no frequency component appear at the same radiator for two different members of the set. A member of such a set, indexed by the parameter  $\gamma$ , is shown in figure #10.

Suppose first that the receiver undergoes a time-integration process also, such that an array at any time is matched to the transmitting array. This means that a given element will accept only the return contribution from the corresponding radiating element. Other contributions can be eliminated on a frequency discrimination basis. Intuitively such a receiver wastes power return, compared to the previous system. Mathematically,  $a_{nm}b_{nl}$  will be zero when  $m \neq l$ , so that the two-way pattern, within a delay, is

$$(5.6) \quad V(t) = C(R, \theta) \sum_n \sum_m a_{nm} b_{nm} e^{j\omega_n \left[ t - \frac{2R}{c} + \frac{2x_m \sin \theta}{c} \right]}$$

Figure 10



MULTIPLE-FREQUENCY ARRAY IN THE  
TIME-INTEGRATION SET



This expression indicates a loss in directivity and a loss in power, by virtue of the fewer number of terms involved. Consequently, this system has limited or no application to radar or sonar.

A second possible receiver is a wide band conventional array, which receives the entire reflected bandwidth at each radiator. The result of applying the time-integration process here can be shown to be the two way pattern of (5.5). Thus, a set of no-gain multiple frequency arrays can be combined with a wide band conventional receiver to yield the two-way pattern of a conventional system.\* In some applications, however, the necessity for having a conventional receiver may be a disadvantage. This is shown next.

### Pattern Rotation

The pattern expression is

$$(5.7) \quad Q(\theta, t - \frac{R}{c}) = \int_{-\infty}^{\infty} \int_{-P}^P A(x, \omega) e^{j\omega(t - \frac{R}{c} + \frac{x}{c} \sin \theta)} dx \frac{d\omega}{2\pi}$$

when  $A(x, \omega)$  is the excitation spectrum. The pattern  $Q(\theta - \theta_0, t - \frac{R}{c})$  is said to be the rotated version of  $Q(\theta, t - \frac{R}{c})$  and is given

approximately by

$$(5.8) \quad Q(\theta - \theta_0, t - \frac{R}{c}) \approx \int_{-\infty}^{\infty} \int_{-P}^P A(x, \omega) e^{-j\frac{\omega x}{c} \sin \theta_0} e^{j\omega(t - \frac{R}{c} + \frac{x}{c} \sin \theta)} dx \frac{d\omega}{2\pi}$$

Thus in order to rotate the pattern  $Q$  (transmit or receive) by  $\theta_0$ , the phase distribution  $e^{-j\frac{\omega x}{c} \sin \theta_0}$  is appended to the excitation

(or filter)  $A(x, \omega)$ . In the time domain the new excitation becomes  $a(x, t - \frac{x}{c} \sin \theta_0)$ .<sup>(9)</sup> Rotation of the two-way pattern re-

quires a similar change in both excitation and filtering functions.

For scanning the quantity  $\theta_0$  will vary with time; so time varying time delays are required for electronic scanning. This operation is difficult to perform in practice, except in the case where  $A(x, w)$  is a narrow-band function. Then a time delay is equivalent to a phase shift which is much easier to implement. For example, the arrays of chapter 3 are amenable to electronic rotation since each element operates at a single frequency.

In the light of these remarks, it follows that when electronic scanning is preferred to mechanical scanning, the time integration process is more efficient for a set of conventional arrays rather than a set of multiple frequency arrays. The latter required the use of a wide band conventional receiver, whose pattern would be difficult to rotate electronically.\*

As a first step in the proof of these assertions, the ambiguity function corresponding to the pattern  $Q(R, \theta)$  is defined as

$$(1.1) \quad \tilde{Q}(R, \Delta\theta) = \text{Re} \int \int Q(R, \theta) Q^*(R + \Delta R, \theta + \Delta\theta) d\theta dR$$

In a sense this quantity indicates the maximum joint resolution possible from a pattern  $Q(R, \theta)$ . From the expression,

$$(1.2) \quad \int \int |Q(R, \theta) - Q(R + \Delta R, \theta + \Delta\theta)|^2 d\theta dR = 2(E - \tilde{Q}(R, \Delta\theta))$$

where  $E$  is the total pattern energy, it is seen that the ambiguity



## CHAPTER 6

## AMBIGUITY FUNCTION

As opposed to the time integration process where a set of transmission patterns are combined, this chapter concerns a pattern transformation, which is known as the "ambiguity function"<sup>10</sup>. Attention is placed on the no-gain multiple frequency array here, for this is an extreme array. The two principle results for these arrays are

- (1) The ambiguity function, for some such arrays can be arbitrarily localized in each of its two degrees of freedom.
- (2) The localization can be realized in practice as if the ambiguity function, with  $R$  and  $\theta$  as the two degrees of freedom, were the actual radiation pattern. Thus a physical realizable processing technique exists which brings out joint directive and range localization although the pattern of no-gain multiple frequency arrays has poor directivity.

As a first step in the proof of these assertions, the ambiguity function corresponding to the pattern  $Q(R, \theta)$  is defined as

$$(6.1) \quad \Phi(\Delta R, \Delta \theta) \equiv R_e \int_{-\infty}^{\infty} \int_0^{2\pi} Q(R, \theta) Q^*(R + \Delta R, \theta + \Delta \theta) d\theta dR$$

In a sense this quantity indicates the maximum joint resolution possible from a pattern  $Q(R, \theta)$ . From the expression,

$$(6.2) \quad \int_{-\infty}^{\infty} \int_0^{2\pi} |Q(R, \theta) - Q(R + \Delta R, \theta + \Delta \theta)|^2 d\theta dR = 2(E - \Phi(\Delta R, \Delta \theta))$$

where  $E$  is the total pattern energy, it is seen that the ambiguity



function measures and represents the degree of pattern difference as a function of separation. This is important for resolution because returned signals are distinguished in relation to their difference. When  $\Phi(\Delta R, \Delta \theta)$  is small (6.2) shows that the pattern  $Q(R, \theta)$  is almost independent of its shifted version,  $Q(R + \Delta R, \theta + \Delta \theta)$ . Consequently the return of a target at the point  $(R, \theta)$  is theoretically distinguishable from a return originating from the point  $(R + \Delta R, \theta + \Delta \theta)$ . Conversely, when  $\Phi(\Delta R, \Delta \theta)$  is large,  $Q(R, \theta)$  and  $Q(R + \Delta R, \theta + \Delta \theta)$  are similar, hence not as easily distinguished in noise. For instance,  $\Phi(0, 0) = E$  is a maximum; the integrated difference in (6.2) is then zero. For resolution, the ideal ambiguity function has become small for small separations  $\Delta R$  and  $\Delta \theta$ .

Now consider excitations of the form  $a(x)e^{jw(x)t}$  where  $w(x)$  never assumes the same value more than once over the array.

The pattern is given by

$$(6.3) \quad Q(R, \theta) = \int_{-P}^P a(x) e^{jw(x)(t - \frac{R}{c} + \frac{x}{c} \sin \theta)} dx$$

Substitution of this quantity into (6.1) results in

$$(6.4) \quad \Phi(\Delta R, \Delta \theta) = \text{Re} \int_{-\infty}^{\infty} dR \int_0^{2\pi} d\theta \int_{-P}^P a(x_1) a(x_2) e^{jw(x_1)(t - \frac{R}{c} + \frac{x_1}{c} \sin \theta)} \cdot e^{-jw(x_2)(t - \frac{R + \Delta R}{c} + \frac{x_2}{c} \sin(\theta + \Delta \theta))} dx_1 dx_2$$

Interchange of the integration order and calculation of the R-integration yields

$$(6.5) \quad \Phi(\Delta R, \Delta \theta) = \text{Re} \int_0^{2\pi} \int_{-P}^P |a(x)|^2 e^{j \frac{w(x) \Delta R}{c}} e^{j \frac{w(x) x}{c} \left[ \sin(\theta - \frac{\Delta \theta}{2}) - \sin(\theta + \frac{\Delta \theta}{2}) \right]} dx d\theta$$

since  $\int_{-\infty}^{\infty} e^{j \frac{R}{c} [w(x_2) - w(x_1)]} dR = \delta[w(x_1) - w(x_2)]$  and  $w(x_1) \neq w(x_2)$  when  $x_1 \neq x_2$ . Using the facts that



$$\sin\left(\theta + \frac{\Delta\theta}{2}\right) - \sin\left(\theta - \frac{\Delta\theta}{2}\right) = 2 \cos\theta \sin \frac{\Delta\theta}{2} \quad \text{and}$$

$$(6.6) \quad \int_0^{2\pi} e^{j\theta \cos\theta} d\theta = 2\pi J_0(\theta)$$

where  $J_0(\theta)$  is the zero order Bessel function, one obtains the final result,

$$(6.7) \quad \Phi(\Delta R, \Delta\theta) = \text{Re} \, 2\pi \int_{-P}^P |a(x)|^2 e^{j \frac{w(x)\Delta R}{c}} J_0\left[\frac{2w(x)x}{c} \sin \frac{\Delta\theta}{2}\right] dx$$

For the ambiguity function a measure of localization in  $\Delta\theta$  can be defined with the same meaning that directive gain has for angular localization in the pattern. Thus let

$$(6.8) \quad H \equiv \frac{\int_0^\infty |\Phi(\Delta R, 0)|^2 d\Delta R}{\frac{1}{2\pi} \int_0^{2\pi} \int_0^\infty |\Phi(\Delta R, \Delta\theta)|^2 d\Delta R d\Delta\theta}$$

be called the ambiguity constant; then the ambiguity constant

can be taken as analogous to the directive gain. Substitution

of (6.7) into (6.8), then use of  $\int_{-\infty}^{\infty} e^{j\frac{\Delta R}{c} [w(x_1) - w(x_2)]} d\Delta R = \delta(x_1 - x_2)$

results in

$$(6.9) \quad H = \frac{\int_{-P}^P |a(x)|^4 dx}{\pi \int_0^\pi \int_{-P}^P |a(x)|^4 J_0^2\left[\frac{2w(x)x}{c} \sin \frac{\Delta\theta}{2}\right] dx d\Delta\theta}$$

This is the ambiguity constant of the no-gain multiple frequency

array, given by the excitation  $a(x)e^{jw(x)t}$ . Since, except for

zero argument, the zero-order Bessel function is always less than

one,  $H > 1$  even though  $G_d = 1$ . Also since the Bessel function

approaches zero for large arguments,  $H$  becomes arbitrarily

large as either the array length,  $2P$ , or the frequencies,  $w(x)$  be-

come large. Thus, at least in theory, the angular resolution

capability of no-gain multiple frequency arrays can be made

arbitrarily good.



The range resolution capability is indicated by setting  $\Delta\theta = 0$  in (6.7). Then

$$(6.10) \quad \Phi(\Delta R, 0) = \operatorname{Re} 2\pi \int_{-P}^P |a(x)|^2 e^{j\frac{\omega(x)\Delta R}{c}} dx$$

which is analogous to the broadside pulse of the pattern. By inspection of expression (3.3), it is seen that (6.10) has the same general form as its corresponding broadside pulse. Consequently the requirement for fine range resolution is the same as before, namely, high total bandwidth over the array. As before the total bandwidth is independent of the individual radiators or path bandwidths. This requirement can be satisfied by merely extending the array length. It follows from this and the consideration of the ambiguity constant that  $\Phi(\Delta R, \Delta\theta)$  can be made arbitrarily localized in  $\Delta\theta$  and  $\Delta R$ .

### Implementation

Suppose that point targets exist at the points  $(R_n, \theta_n)$  for  $n = 1, 2, \dots, N$ . From (2.11) it is seen that the two-way pattern has the form  $V(\theta, t - \frac{2R}{c})$ ; so the received signal is given by

$$(6.11) \quad S(t) = \sum_{n=1}^N V(\theta_n, t - \frac{2R_n}{c})$$

Incorporating the second degree of freedom, pattern rotation, the received signal will depend on the amount of pattern rotation. This may be written as

$$(6.12) \quad S(t, \alpha) = \sum_{n=1}^N V(\theta_n - \alpha, t - \frac{2R_n}{c})$$

The quantity of interest is the two dimensional correlation function given by

$$(6.13) \quad \begin{aligned} r(\Delta\theta, \Delta R) &= \int_0^{2\pi} \int_{-\infty}^{\infty} V^*(\Delta\theta - \alpha, t - \frac{2\Delta R}{c}) S(t, \alpha) dt d\alpha \\ &= \sum_{n=1}^N \int_0^{2\pi} \int_{-\infty}^{\infty} V^*(\Delta\theta - \alpha, t - \frac{2\Delta R}{c}) V(\theta_n - \alpha, t - \frac{2R_n}{c}) dt d\alpha \end{aligned}$$



where  $\Delta\theta$  and  $\Delta R$  are arbitrarily specified.

Suppose that the two-way pattern  $V(\theta, t - \frac{2R}{c})$  is the combined effect of a transmitter with excitation  $a_0(x)e^{j\omega(x)t}$ , describing a no-gain multiple frequency array, and a wide-band non-directive receiver. Suppose the filters following the array points are given by  $b(y)$  for all frequencies transmitted.

Then by (2.11)

$$(6.14) \quad V(\theta, t - \frac{2R}{c}) = \iint_{-P}^P b(y) a_0(x) e^{j\omega(x)(t - \frac{2R}{c} + \frac{x+y}{c} \sin\theta)} dx dy$$

$$= \int_{-P}^P a(x) e^{j\omega(x)(t - \frac{2R}{c} + \frac{x}{c} \sin\theta)} dx$$

where

$$(6.15) \quad a(x) = a_0(x) \int_{-P}^P b(y) e^{j\frac{\omega(x)}{c} y \sin\theta} dy$$

is just some function of  $x$ . This is valid since the receiver pattern is assumed non-directive. Therefore by (6.3)

$$(6.16) \quad V(\theta, t - \frac{2R}{c}) = Q(2R, \theta)$$

By using (6.16) and (6.1) one obtains for (6.13)

$$(6.17) \quad \Gamma(\Delta\theta, \Delta R) = \sum_{n=1}^N \Phi(\Delta\theta - \theta_n, 2[\Delta R - R_n])$$

which is the desired result.

This result means that for such a system, each point target will ultimately produce in the received signal the ambiguity function centered about the point  $(\alpha, t)$  corresponding to the target location. It was shown previously that the no-gain multiple frequency array ambiguity function can be made arbitrarily localized about its maximum value. For these situations the various "ambiguity returns" can be distinguished in noise for any separations which are not small. Hence an operation has been shown which

derives the full theoretical resolution indicated by a particular ambiguity function.

To determine the practicality of the system a close examination of its constituents is necessary. The main constituents are a no-gain multiple frequency array transmitter, a non-directive receiver, and a two-dimensional correlator. Although there will be mutual coupling on transmission both the transmit and receive arrays can be built without unusual problems. In fact, as noted before, the implementation of electronic pattern rotation is greatly facilitated by the use of these arrays. It may seem, secondly, that the system will waste energy since it utilizes non-directive arrays. This, however, is false. Any target, regardless of its location and pattern rotation  $\alpha$ , reflects the same amount of transmitted energy since the pattern is non-directive. Likewise, on reception each return is accepted with the same weighting regardless of its origination because again the pattern is non-directive. Hence there is no chance to waste energy on transmission or reception. It is true that for several targets the received signal will be unintelligible; nevertheless a means has been devised above to unscramble the received signal.

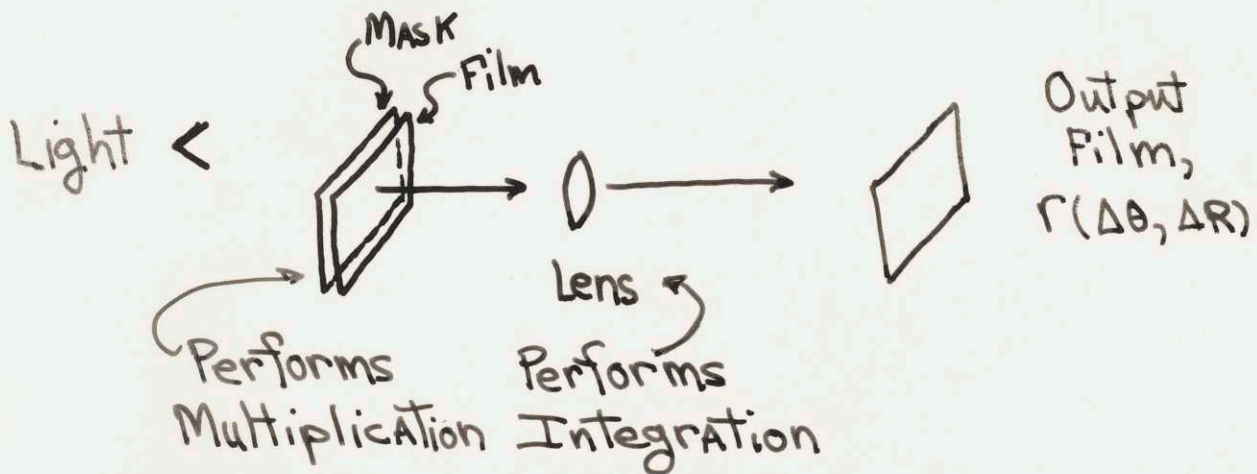
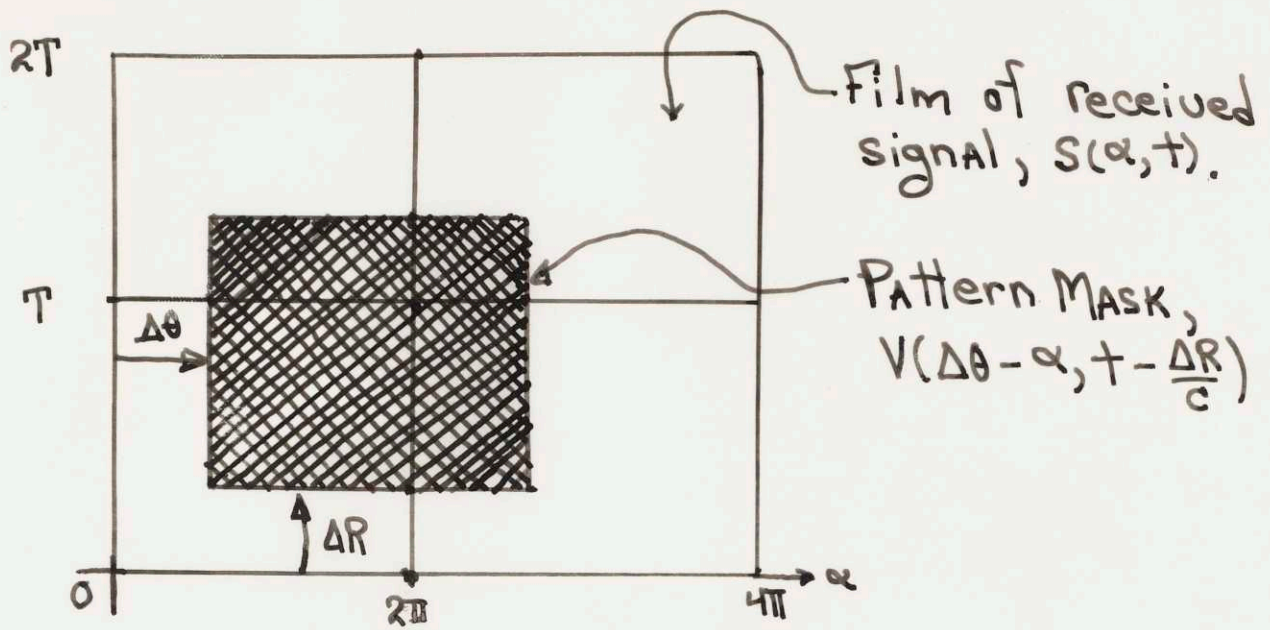
The major difficulty arises in instrumenting the two-dimensional correlator of (6.13). One proposed solution was to use optical processing techniques. Here the signal return is initially converted into a two-dimensional film having the same amplitude variation as  $s(x,t)$ . A masking film having the amplitude of the known pattern  $V(\theta, t - \frac{R}{c})$  can be superimposed



for multiplication, and integrations can be performed by lenses.<sup>11</sup> The scanning of the mask which accounts for the various values of  $\Delta R$  and  $\Delta \theta$  in (6.13) can be performed mechanically. Of course in practice the rotation parameter  $\alpha$  can take on only discrete values, so that results will be approximate. To a good approximation, however, the final result will be a new film having the same amplitude variation as  $r(\Delta R, \Delta \theta)$ . A pictorial representation of the process is given in figure #11. Another technique uses straight forward electronic processing, which, however, requires a great deal of computation. Figure #12 outlines this technique.

In either case the implementation is involved and complex. This complexity is the main sacrifice for obtaining the increased resolution capability of the ambiguity function. As shown in the next chapter, this problem is compounded when the targets are non-stationary.

Figure 11

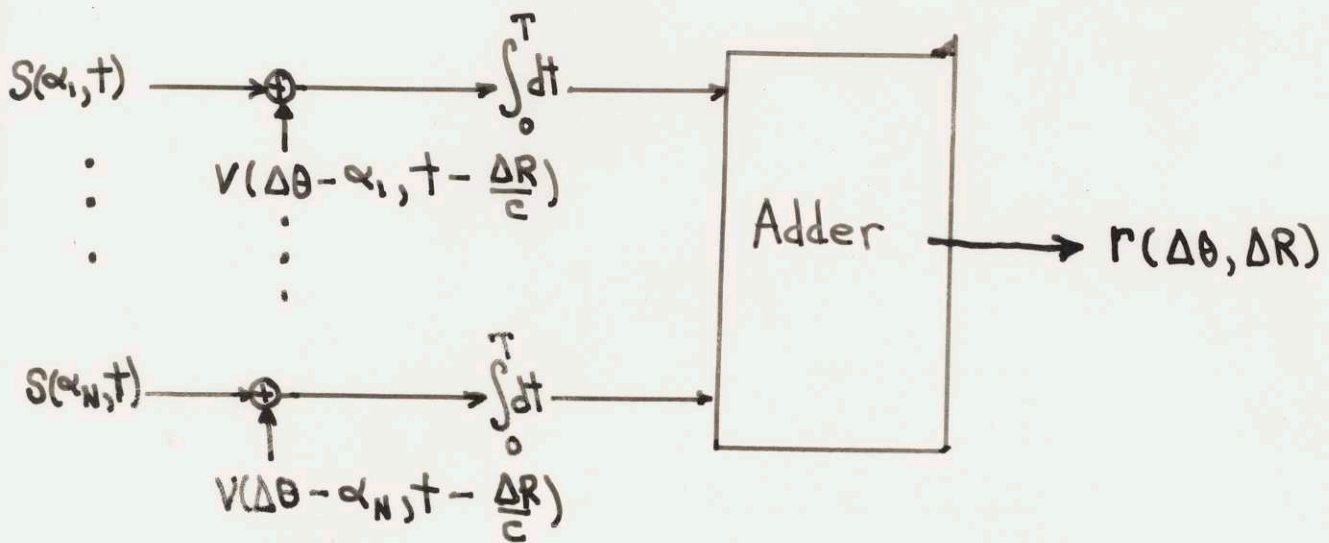


AMBIGUITY FUNCTION PROCESSOR  
(optical)



The EQUATION TO BE INSTRUMENTED is

$$\int_0^T \sum_{i=1}^N S(\alpha_i, t) V(\Delta\theta - \alpha_i, t - \frac{\Delta R}{c}) dt = r(\Delta\theta, \Delta R)$$



AMBIGUITY FUNCTION PROCESSOR  
(electronic)

## CHAPTER 7

## DOPPLER EFFECTS

This final chapter describes the effect of radial target velocity on the pattern and the ambiguity function of an array. The results are based on the doppler effect which states that a reflector moving with velocity  $v$  reflects an ingoing signal  $ae^{j\omega t}$  as  $ae^{j\omega(1+\frac{v}{c})t}$  for any frequency  $\omega$ . If the ingoing signal is given by

$$(7.1) \quad a(t) = \int_{-\infty}^{\infty} A(\omega) e^{j\omega t} \frac{d\omega}{2\pi}$$

the effect will be a transformation into the new signal,

$$(7.2) \quad a'(t) = \int_{-\infty}^{\infty} A(\omega) e^{j\omega[1+k]t} \frac{d\omega}{2\pi} = \int_{-\infty}^{\infty} \frac{A(\frac{\omega}{1+k})}{1+k} e^{j\omega t} \frac{d\omega}{2\pi}$$

where  $k = \frac{v}{c}$ . Hence the original spectrum  $A(\omega)$  changes to  $\frac{A(\frac{\omega}{1+k})}{1+k}$  upon reflection off the moving reflector. Since  $k$  is always small this may be approximated by  $A[\omega(1-k)]$ .

Taking the transmission pattern to mean the reflected signal as a function of reflector location, the expression accounting for doppler effects may be written

$$(7.3) \quad Q(\theta, t - \frac{R}{c}) = \int_{-\infty}^{\infty} \int_{-P}^P A[x, (1-k)\omega] e^{j\omega(t - \frac{R}{c} + \frac{x}{c} \sin\theta)} dx \frac{d\omega}{2\pi}$$

This applies only to transmission patterns since the receivers experience no doppler effects, and hence their pattern form is unchanged. Therefore the two-way pattern for the filter function  $B(x', \omega)$  can be written

$$(7.4) \quad V(\theta, t - \frac{R}{c}) = \int_{-\infty}^{\infty} \frac{d\omega}{2\pi} \int_{-P}^P A[x, \omega(1-k)] B(x', \omega) e^{j\omega(t - \frac{2R}{c} + \frac{x+x'}{c} \sin\theta)} dx dx'$$

As long as the effective bandwidths of the receiver filters are large enough to accept the frequency shifted returns, directivity



and range localization are unchanged by doppler effects. The amount of frequency duplication and the bandwidth of  $A(x, w)$  are the same in (7.4). Also the method derived for pattern rotation is still valid.

Finally <sup>it</sup> is desired to find the effect of target velocity on the system of the preceding chapter. In that case  $A(x, w) = a(x) \delta[w - w(x)]$  so that

$$(7.5) \quad A(x, w(1-k)) = a(x) \delta[w(1-k) - w(x)]$$

Therefore, after using (6.14), (7.4), and (7.5), the two-way pattern is written

$$(7.6) \quad V(\theta, t - \frac{2R}{c}) = \int_{-P}^P a(x) e^{jw(x)(1+k)(t - \frac{2R}{c} + \frac{x}{c} \sin \theta)} dx$$

Assuming for simplicity there is a target at (0,0), the operation of (6.13) becomes for  $\Delta \theta = 0$ ,

$$(7.7) \quad \Gamma(\Delta R, 0) = \text{Re} \int_{-\infty}^{\infty} dR \int_0^{2\pi} d\theta \iint_{-P}^P a(x_1) a^*(x_2) e^{jw(x_1)(1+k)(t - \frac{2R}{c})} \cdot e^{-jw(x_2)(t - \frac{2R + \Delta R}{c})} e^{j \sin \theta \left( \frac{x_1 w(x_1)(1+k)}{c} - \frac{x_2 w(x_2)}{c} \right)} dx_1 dx_2$$

Having performed the  $R$  and  $\theta$  integrations,

$$(7.8) \quad \Gamma(\Delta R, 0) = 2\pi \text{Re} \iint_{-P}^P dx_1 dx_2 a(x_1) a^*(x_2) \delta[w(x_1)(1+k) - w(x_2)] e^{j \frac{w(x_2) \Delta R}{c}} \int_0^{2\pi} d\theta \left[ \frac{w(x_1) x_1 (1+k)}{c} - \frac{x_2 w(x_2)}{c} \right]$$

The delta function establishes a relation between the variables of integration,  $x_1$ , and  $x_2$ , which can be written

$$(7.9) \quad x_1 = f(x_2) \equiv w^{-1} \left[ \frac{w(x_2)}{1+k} \right]$$

when  $w^{-1}(y)$  is the inverse function of  $w(x)$ . Note that such an inverse exists for no-gain multiple frequency arrays since no frequency is duplicated along the array. Using (7.9) there results

$$(7.10) \quad \Gamma(\Delta R, 0) = 2\pi \text{Re} \int_{-P}^P a(x) a^*[f(x)] e^{j \frac{w(x) \Delta R}{c}} \int_0^{2\pi} d\theta \left[ \frac{w(x)}{c} (f(x) - x) \right] dx$$

Comparing this result with (6.10) (when  $k = 0$ ), two

observations can be made. First, the factor of the Bessel function has an attenuating effect on the pulse. Second, the factor  $a[f(x)]$  is zero for some interval of  $x$  within the interval  $(-P, P)$ . If for instance  $k$  is positive,  $\frac{\text{minimum } w(x)}{1+k}$  will be smaller than any  $w(x)$ ; consequently  $f(x_0)$  lies outside the interval  $(-P, P)$  and  $a(f(x_0)) = 0$  since  $a(x) = 0$  for  $|x| > P$ . When the entire interval of integration is not used, the bandwidth corresponding to the factor  $e^{jw(x)} \Delta R$  is diminished. As has been demonstrated, this bandwidth loss is equivalent to a loss in range resolution.

This provides sufficient information to conclude that the system of chapter 6 has been distorted by doppler effects. The extent of this distortion as a function of  $k$  is still an open question since the mathematics becomes involved. Presumably, however, directive distortion occurs also. To compensate for the distortion it is possible to have numerous doppler channels so that a given return is correlated with the proper doppler shifted pattern. The number of channels required depends on the doppler resolution desired and the ambiguity distortion which will be tolerated. This solution to the problem, of course, compounds the problem of equipment complexity which was discussed in chapter 6.



## CHAPTER 8

## SUMMARY

The utility of multiple frequency arrays, as discussed in this paper, has been determined for three types of radar systems. The first is the usual type of system requiring directive and very localized energy emission from the array. The relation between the excitation (or filtering) function and the relative joint satisfaction of these two requirements appeared in expression (4.19). Prior to stating that expression, the directive gain was shown to be a measure of pattern directivity, and the effective bandwidth, a measure of pattern range localization. The fundamental statement (4.19) established the gain-bandwidth product. In the case of a conventional array the product was separable; this means that here directivity and range resolution are independent entities, limited, if at all, independently.

In the case of a multiple frequency array the gain-bandwidth product was a single entity, constrained by the composite gain. The composite gain was shown to measure the frequency-position area in the excitation spectra. Therefore an antenna excitation with a certain total output bandwidth and array length, has the greatest gain-bandwidth product for a conventional array. Such an array excitation uses the entire output bandwidth at each array point, so its consequent composite gain is largest.

Physically, it is more natural to constrain the bandwidth of the individual radiators than it is to constrain the ef-

fective length of each frequency component in the excitation. This consideration leads to another point of view. Suppose first there is a constraint on the overall length of a multiple frequency array. As shown in (4.16) the directivity of the array is an average of the directivities of the constituent monochromatic conventional arrays. Since the effective length of each constituent is less than that of the entire array, a directivity reduction is implied. The conventional array, on the other hand, is composed of monochromatic conventional arrays each having the same effective length. Thus, here no directivity reduction is involved; so in the context of these two considerations it behooves one to use the conventional array.

Now suppose the excitation bandwidths at each array point is constrained below some desired output bandwidth. A multiple frequency array will enable the desired output bandwidth to be reached, though as before the effective array length will be less than the actual length. Finally when the constraint of a fixed array length is dropped, the effective length or gain of the array can be achieved by extending the array. The practicality of these constraints will depend on the actual application.

The second system to be considered was the time-integration process employing discrete arrays. Here a set of no-gain multiple frequency array were combined in such a way to produce the two-way pattern of a wide-band conventional array. The great advantage of using multiple frequency arrays rather than monochromatic conven-



tional arrays is the possibility of using an envelope detector on reception. For a set of conventional arrays the RF phase would matter; for the multiple frequency array it would not matter. The relative disadvantage in using the system was the difficulty of implementing an electronic scanning scheme on reception, though no such problem existed on transmission.

The final system made use of a type of correlation processing to achieve joint angular and radial resolution from a no-gain multiple frequency array. The process could just as well <sup>have</sup> been applied to the conventional array, and sample calculations show that the joint resolution would be better. The unique feature of the multiple frequency array in this application is the very low bandwidth output from each individual radiator. If for instance a monochromatic conventional array were used instead, no radial resolution would be possible; whereas the multiple frequency array ambiguity function can achieve arbitrarily good joint resolution. The advantage in having excitations consisting of a single frequency at each radiator appears as the great facility in instrumenting pattern rotation schemes. The major problem for the system was the complexity in the implementation of a two-dimensional correlator.

Two unexplored questions arise. First, can simplifications in the ambiguity systems be obtained through the use of multiple frequency arrays having some directive gain? Second, can acceptable degrees of doppler resolution, together with range and angle resolution be obtained with the "ambiguity function" system?

## BIBLIOGRAPHY

1. S. Silver, "Microwave Antenna Theory and Design," Radiation Laboratory Series No. 12, Mc-Graw Hill, New York; chap. 5,6; 1949.
2. S. Mason and H. Zimmerman, "Electronic Circuits, Signals, and Systems," John Wiley and Sons, New York; p. 236; 1960.
3. S. A. Schelkinoff and H. T. Friis, "Antennas Theory and Practice", John Wiley and Sons, New York; Chap. 6; 1952.
4. E. Jahnke and F. Emde, Tables of Functions, Fourth Edition, Dover Publications, New York; pp. 34-37; 1945.
5. N. Wiener; "The Fourier Integral and Certain of its Applications"; Dover Publications, New York; Chap. 1, 2; 1933.
6. H. Urkowitz, C. Hauer, and J. F. Koval; "Generalized Resolution in Radar Systems"; Proceeds of the IRE, Vol. 50, No. 10, 1960.
7. T. K. Kashihara, "Investigation of Advanced Antenna Techniques", Philco Scientific Laboratory, Blue Bell, Pa., AF 19 (628) - 2403, Status Report 1; March 1963.
8. L. J. Cutrona, E. N. Leith, C. J. Palermo, and L. S. Porcello, "Optical Data Processing and Filtering Systems", IRE Transactions on Information Theory; June, 1960.